

# Nutrient release and flux dynamics of CO<sub>2</sub>, CH<sub>4</sub>, and N<sub>2</sub>O in a coastal peatland driven by actively induced rewetting with brackish water from the Baltic Sea

Daniel Lars Pönisch<sup>1\*</sup>, Anne Breznikar<sup>2\*</sup>, Cordula Nina Gutekunst<sup>3</sup>, Gerald Jurasinski<sup>3</sup>, Maren Voss<sup>2</sup>,  
5 Gregor Rehder<sup>1</sup>

*\* these authors contributed equally to this work and share first authorship*

<sup>1</sup> Department of Marine Chemistry, Leibniz Institute for Baltic Sea Research Warnemünde (IOW), Rostock, Germany

<sup>2</sup> Department of Biological Oceanography, Leibniz Institute for Baltic Sea Research Warnemünde (IOW), Rostock, Germany

<sup>3</sup> Department of Landscape Ecology, Faculty for Agriculture and Environmental Sciences, University of Rostock, Germany

10 Correspondence to: Daniel L. Pönisch (daniel.poenisch@io-warnemuende.de) and Anne Breznikar (anne.breznikar@io-warnemuende.de)

**Abstract.** The rewetting of drained peatlands supports long-term nutrient removal in addition to reducing emissions of carbon dioxide (CO<sub>2</sub>) and nitrous oxide (N<sub>2</sub>O). However, rewetting may lead to short-term nutrient leaching into adjacent water and high methane (CH<sub>4</sub>) emissions. The consequences of rewetting with brackish water on nutrient and greenhouse gas (GHG)  
15 fluxes remain unclear, although beneficial effects such as lower CH<sub>4</sub> emissions seem likely. Therefore, we studied the actively induced rewetting of a coastal peatland with brackish water, by comparing pre- and post-rewetting data from the peatland and the adjacent bay.

Both the potential transport of nutrients into adjacent coastal water and the shift of GHG fluxes (CO<sub>2</sub>, CH<sub>4</sub>, N<sub>2</sub>O) accompanying the change from drained to inundated conditions were analyzed based on measurements of the surface water  
20 concentrations of nutrients (dissolved inorganic nitrogen (DIN), phosphate (PO<sub>4</sub><sup>3-</sup>)), oxygen (O<sub>2</sub>), components of the CO<sub>2</sub> system, CH<sub>4</sub>, and N<sub>2</sub>O together with manual closed-chamber measurements of GHG fluxes.

Our results revealed higher nutrient concentrations in the rewetted peatland than in the adjacent bay, indicating that nutrients leached out of the peat and were exported to the bay. A comparison of DIN concentrations of the bay with those of an unaffected reference station showed a significant increase after rewetting. The maximum estimated nutrient export (mean  
25 ± 95 % confidence level) out of the peatland was calculated to be 33.8 ± 9.6 t yr<sup>-1</sup> for DIN-N and 0.24 ± 0.29 t yr<sup>-1</sup> for PO<sub>4</sub>-P, depending on the endmember (bay vs. reference station).

The peatland was also a source of GHG in the first year after rewetting. However, the spatial and temporal variability decreased and high CH<sub>4</sub> emissions, as reported for freshwater rewetting, did not occur. CO<sub>2</sub> fluxes (mean ± SD) decreased slightly from 0.29 ± 0.82 g m<sup>-2</sup> h<sup>-1</sup> (pre-rewetting) to 0.26 ± 0.29 g m<sup>-2</sup> h<sup>-1</sup> (post-rewetting). The availability of organic matter  
30 (OM) and dissolved nutrients were likely the most important drivers of continued CO<sub>2</sub> production. Pre-rewetting CH<sub>4</sub> fluxes ranged from 0.13 ± 1.01 mg m<sup>-2</sup> h<sup>-1</sup> (drained land site) to 11.4 ± 37.5 mg m<sup>-2</sup> h<sup>-1</sup> (ditch). After rewetting, CH<sub>4</sub> fluxes on the

formerly dry land increased by one order of magnitude ( $1.74 \pm 7.59 \text{ mg m}^{-2} \text{ h}^{-1}$ ), whereas fluxes from the former ditch decreased to  $8.5 \pm 26.9 \text{ mg m}^{-2} \text{ h}^{-1}$ . These comparatively low  $\text{CH}_4$  fluxes can likely be attributed to the suppression of methanogenesis and oxidation of  $\text{CH}_4$  by the available  $\text{O}_2$  and sulfate in the rewetted peatland, which serve as alternative electron acceptors. The post-rewetting  $\text{N}_2\text{O}$  flux was low, with an annual mean of  $0.02 \pm 0.07 \text{ mg m}^{-2} \text{ h}^{-1}$ .

Our results suggest that rewetted coastal peatlands could account for high, currently unmonitored nutrient inputs into adjacent coastal water, at least on a short time scale such as a few years. However, rewetting with brackish water may decrease GHG emissions and might be favored over freshwater rewetting in order to reduce  $\text{CH}_4$  emissions.

## 1. Introduction

Pristine peatlands are natural sinks for nutrients, in particular nitrate ( $\text{NO}_3^-$ ), and greenhouse gases (GHG) such as mostly carbon dioxide ( $\text{CO}_2$ ) and occasionally nitrous oxide ( $\text{N}_2\text{O}$ ) (Martikainen et al., 1993; Regina et al., 1996; Strack, 2008; Kaat and Joosten, 2009). Globally, peatlands store up to 550 Gt of carbon (C), which is twice the C stock of total forest biomass (Moore et al., 1998; Joosten and Clarke, 2002; Kaat and Joosten, 2009).

The drainage of peatlands leads to the mineralization of the topmost peat layer and the accumulation of nutrients (Smolders et al., 2006; Geurts et al., 2010). After rewetting, peatlands can therefore be sources of nutrients, especially ammonium ( $\text{NH}_4^+$ ) and phosphate ( $\text{PO}_4^{3-}$ ) (Lamers et al., 2002; Duhamel et al., 2017). Conversely, due to the anoxic conditions in the water-saturated peat, rewetted peatlands can also act as nutrient sinks, mainly for  $\text{NO}_3^-$  (Fisher and Acreman, 2004). Whether rewetting leads to nutrient release or uptake is, besides other factors, controlled by the degree of peat decomposition (Zak and Gelbrecht, 2007; Cabezas et al., 2012), the water level (Duhamel et al., 2017) and the salinity (Liu and Lennartz, 2019). Nutrient release is highest in strongly degraded peat in formerly drained peatlands (Zak and Gelbrecht, 2007; Cabezas et al., 2012). Therefore, removal of the topsoil before rewetting has been recommended as a measure to greatly reduce the release of  $\text{PO}_4^{3-}$  and nitrogen (N) (Harpenslager et al., 2015; Zak et al., 2017). However, nutrient release from peat after rewetting has mostly been assessed in laboratory and incubation studies. To our knowledge, field data on nutrient leaching and potential exports to adjacent waters are lacking.

The GHG exchange of peatlands is strongly influenced by the prevailing biogeochemical and physical conditions, which in turn are largely determined by vegetation and the water level and thus the ratio of oxic and anoxic conditions (Kaat and Joosten, 2009). In drained peatlands, the low water table enables the aerobic decomposition of peat, which is accompanied by increased  $\text{CO}_2$  emissions (Joosten and Clarke, 2002). In rewetted peatlands,  $\text{CO}_2$  emissions are regulated by photosynthesis, decomposition, and temperature within the upper oxygen-rich soil layer and the overlying water column (Parish, 2008; Oertel et al., 2016). In the anoxic water-saturated zones, the formerly oxygen-induced decomposition of organic matter (OM) is slowed down and relies on alternative terminal electron acceptors (TEAs) such as  $\text{NO}_3^-$ , manganese ( $\text{Mn}^{4+}$ ), iron ( $\text{Fe}^{3+}$ ), and sulfate ( $\text{SO}_4^{2-}$ ), leading to lowered  $\text{CO}_2$  emissions (Strack, 2008; Dean et al., 2018). However, methanogenesis, as the last step in the mineralization of OM and a depletion of TEAs, may become more important in anoxic zones.

Methane (CH<sub>4</sub>) emissions in drained peatlands are virtually negligible at water levels < 20 cm below the surface  
65 (Jurasinski et al., 2016). Although CH<sub>4</sub> is formed in anoxic zones via methanogenesis, most of it is oxidized as it passes through  
the oxic soil layer (Kaat and Joosten, 2009; Dean et al., 2018). Consequently, drained peatlands are a minor source of  
atmospheric CH<sub>4</sub>. In rewetted peatlands, CH<sub>4</sub> is microbially produced in water-saturated, anoxic soil layers mainly by archaea,  
when all other TEAs are depleted (Schönheit et al., 1982; Oremland, 1988; Segers and Kengen, 1998), so that rewetted  
peatlands are often significant sources of CH<sub>4</sub> (Hahn et al., 2015). However, in coastal peatlands that receive marine water and  
70 therefore SO<sub>4</sub><sup>2-</sup>, the contribution of methanogenesis might be reduced, as methanogenic archaea are outcompeted by sulfate-  
reducing bacteria (SRB) (Bartlett et al., 1987; Capone and Kiene, 1988; Oremland, 1988; Jørgensen, 2006). Additionally, any  
CH<sub>4</sub> produced may be oxidized by anaerobic methane oxidation coupled to SO<sub>4</sub><sup>2-</sup> reduction (e.g. Boetius et al., 2000).

N<sub>2</sub>O is an intermediate in microbial processes, mostly nitrification, denitrification and nitrifier-denitrification (Kool  
et al., 2011). In degraded peatlands, all of these processes are fueled by the accumulated nutrients. Drained peatlands can be  
75 weak (Martikainen et al., 1993) or strong sources of N<sub>2</sub>O (Liu et al., 2019), depending mainly on the climate zone and land  
use (Petersen et al., 2012; Leppelt et al., 2014). Rewetted, and thus water-saturated, peat usually acts as N<sub>2</sub>O sink over long-  
term scales, due to the formation of anoxic zones where N<sub>2</sub>O is consumed (Strack, 2008). However, rewetting can at least  
temporarily increase the N<sub>2</sub>O production and thus its release into the atmosphere due to the high nutrient availability in strongly  
degraded peat, which enables higher rates of nitrification and denitrification (Moseman-Valtierra et al., 2011; Chmura et al.,  
80 2016; Roughan et al., 2018).

In temperate latitudes, coastal peatlands are widespread at the interface between marine and terrestrial ecosystems.  
However, for many coastal peatlands, the sinking of their ground level due to degradation and peat shrinkage over decades has  
made them vulnerable to rising sea level and sinking coasts (Jurasinski et al., 2018). In Mecklenburg-Vorpommern  
(northeastern Germany), currently drained coastal peatlands along the low-lying coastline cover an area of ~360–400 km<sup>2</sup>  
85 (Bockholt, 1985; Holz et al., 1996). Nowadays, peatlands are rewetted to restore their habitat function and biodiversity, thereby  
preventing CO<sub>2</sub> and N<sub>2</sub>O emissions and, in the long-term, reestablishing their C- and N-storage capacity (Strack, 2008;  
Zielinski et al., 2018).

Coastal drained peatlands may be rewetted in different ways depending on the available water source. The rewetting  
can consist of permanent flooding with freshwater (from groundwater or rivers), episodic inundations with brackish water  
90 and permanent brackish water flooding. While the effects of freshwater rewetting (Richert et al., 2000; Hogan et al., 2004; Zak  
and Gelbrecht, 2007) and episodic inundations with brackish water on nutrient dynamics and GHG have been investigated  
(Chmura et al., 2011; Neubauer et al., 2013; Hahn et al., 2015; Koebisch et al., 2019), less is known about the impact of  
permanent brackish water flooding.

In this study we examined the immediate effects of rewetting with brackish water on nutrient (NO<sub>3</sub><sup>-</sup>, nitrite (NO<sub>2</sub><sup>-</sup>),  
95 NH<sub>4</sub><sup>+</sup> and PO<sub>4</sub><sup>3-</sup>) and GHG fluxes (CO<sub>2</sub>, CH<sub>4</sub>, N<sub>2</sub>O) in a low-lying, highly degraded coastal peatland at the German Baltic Sea  
coast, by comparing pre- and post-rewetting conditions. Due to the unique formation of a permanent brackish water column  
above formerly drained peat, this is the first study to combine marine shallow-water and terrestrial peatland research. We

investigated how the rewetting with brackish water affects (1) nutrient leaching and the potential transport from a nutrient-enriched, flooded peatland to the adjacent bay driven by frequent water exchange, (2) the GHG dynamics in the surface water within the first year after rewetting and (3) the GHG fluxes along the transition from drained to inundated conditions.

## 2. Material and methods

### 2.1 Study area

The study area is a low-lying, highly degraded coastal peatland that had been transformed from a drained, agriculturally used polder to a brackish wetland. The “Polder Drammendorf” (referred to in the following as “peatland”) is located at the northeastern German Baltic Sea coast, on the western part of the island of Rügen (Mecklenburg-Vorpommern, Germany), bordering on the Kubitzer Bodden (Figure 1). The climate is oceanic, with a mean annual air temperature of 9.1 °C and a mean annual precipitation height of 626 mm (Deutscher Wetterdienst (DWD), 1991–2020). The central Kubitzer Bodden has a mean surface water temperature of  $11.4 \pm 6.6$  °C and a mean surface salinity of  $8.5 \pm 1.4$  (referred to in the following as “central bay”, data retrieved from a monitoring station of the Landesamt für Umwelt, Naturschutz und Geologie Mecklenburg Vorpommern (LUNG MV), 2006–2020, 54.40° N, 13.11° E, Figure 1b). For comparison, the Arkona Basin, the near-by open Baltic Sea basin to the north of the island of Rügen that influences the water in the Kubitzer Bodden, has a mean surface water temperature of  $10.2 \pm 5.6$  °C and a mean surface salinity of  $8.0 \pm 0.5$  (MARNET, data originator: Leibniz Institute for Baltic Sea Research Warnemünde, Germany, 2006–2020, 54.88° N, 13.86° E).

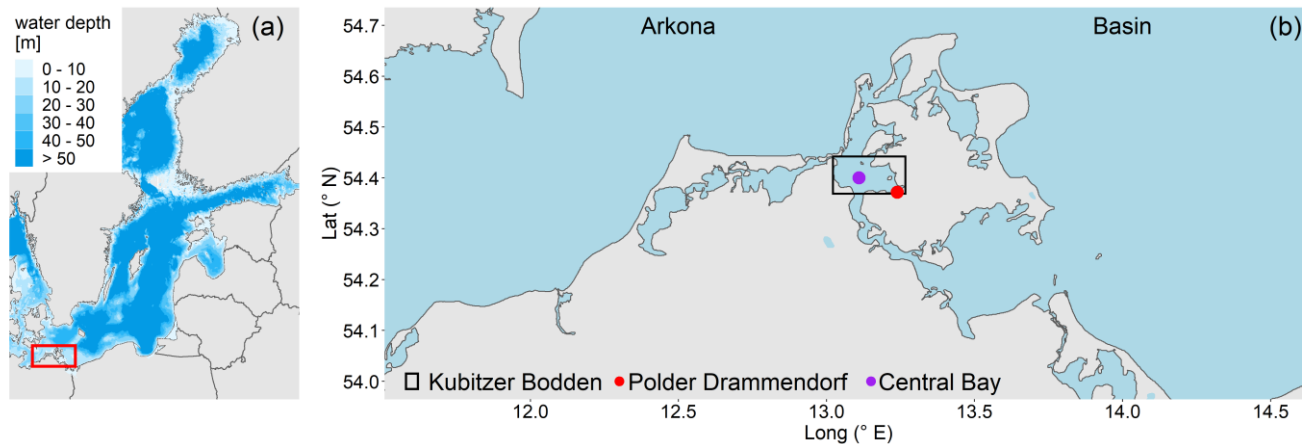
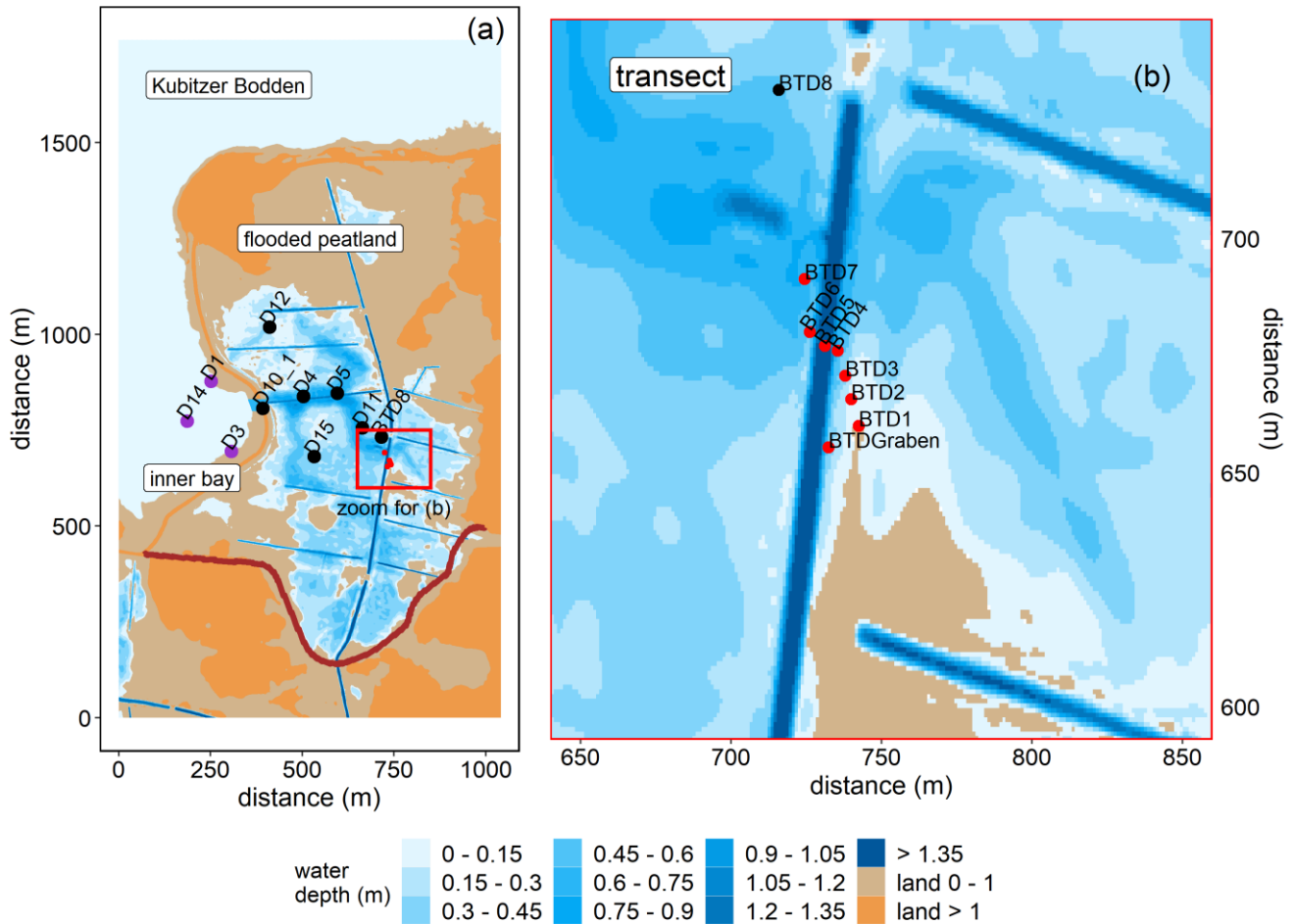


**Figure 1.** (a) Overview of the study area located in the southern Baltic Sea. (b) Coastline of northeast Germany in Mecklenburg-Vorpommern and study area location (“Polder Drammendorf”, red) on the island of Rügen, bordering on the Kubitzer Bodden, where a monitoring station served as reference (“central bay”, purple). The Kubitzer Bodden is connected with the Arkona Basin in the north. Bathymetry refers to Seifert et al., (2001), and borders were retrieved from National Oceanic And Atmospheric Administration (NOAA) - National Centers For Environmental Information (NCEI).

Like most peatlands in northern Germany, Drammendorf was artificially drained for agricultural use (pasture and grassland) in the 1960s, by establishing a sandy dike and an extensive ditch system that affected an area of  $\sim 2.2$  km<sup>2</sup>. The northwestern

part (mostly mineral soil, higher elevation) served as grassland while the northeastern part was used for agriculture with seasonal fertilizer application only until the 1990s ( $100 \text{ kg N ha}^{-1} \text{ yr}^{-1}$ ). The southern compartment (organic soil) provided an area for cattle grazing ( $\sim 30$  cows). The topsoil of the central part consists of up to 50–70 cm highly degraded peat (Brisch, 2015), classified as H7 according to the von Post humification scale (Wang et al., 2021). This highly degraded topsoil layer was not removed prior to rewetting. Underneath the degraded topsoil follows a well-preserved peat layer with a thickness of  $\sim 100$  cm. Peat deposits of up to 220 cm thickness are largest in the western part, near the former dike. The long-lasting drainage and ongoing peat degradation have led to the formation of a local land depression with an average soil elevation of around  $-0.5$  meters above sea level (masl). To control the water expansion after rewetting, a new dike was built in the southern part before flooding (Figure 2a). Additionally, a drainage ditch that receives water from the catchment was rebuilt and a new pumping station was installed. A significant input of nutrients from this additional water supply can be excluded due to the low pumping activity and the absence of a permanent hydrological connection to the study area (Wasser- und Bodenverband Rügen (WBV), pers. comm., 2020).



135 **Figure 2.** Topography of the study area and overview of the stations in the inner bay (purple), the flooded peatland (black)  
and along the transect of the GHG flux measurements (red). (a) Water coverage at mean sea level. The new dike is shown in  
dark red. (b) Transect stations that were sampled for atmospheric chamber-based GHG flux measurements (before and after  
rewetting) and for surface water GHG concentration measurements (after rewetting). Data from station BTD7 were used for a  
comparison of the chamber-based measurements with the calculated air-sea fluxes after rewetting. Topography data retrieved  
140 from the Landesamt für innere Verwaltung MV, Amt für Geoinformation, Vermessungs- und Katasterwesen, Fachbereich  
Geodatenbereitstellung.

The area was rewetted by the targeted removal of a 20 m wide dike section in November 2019 that caused an immediate  
flooding of the low-lying area behind the dike. The newly built channel represents the only permanent hydrological connection  
145 between the peatland and the Kubitzer Bodden that allows major surface water exchange. The remaining section of the dike  
(~650 m) was removed down to the surface elevation level and is hence only flooded at very high water levels.

The restored area covers ~0.8 km<sup>2</sup> in total and is characterized by a permanently water-covered area of ~0.5 km<sup>2</sup>, with  
a mean water depth of ~0.5 m, compared to 1.0–1.5 m in the Kubitzer Bodden. The extent of the inundated area depends  
directly on the water level of the Baltic Sea, which is highly dynamic despite the absence of regular tides (Figure A1).  
150 Therefore, minor changes in the water level lead to major changes in the water-covered area. For instance, if the water level  
rises from –0.5 to + 0.5 masl, the water-covered area increases from 0.08 to 0.7 km<sup>2</sup> (Figure A2, Figure A3). The ditch system  
was only partly removed and hence, some deeper areas with water depths of up to 4 m remained. It is noteworthy that in the  
first months after rewetting, former grassland and ditch vegetation (*Elymus repens* L. (Gould) (Couch grass), *Phragmites*  
*australis* (Cav.) Trin. ex Steud. (Common reed)) died almost completely and the cover of emergent macrophytes was then  
155 negligible. However, *Phragmites* was able to grow back during the growing season and expanded especially around the ditches.

## 2.2 Sampling

### 2.2.1 Surface water sampling

Before rewetting, surface water samples for nutrients (NO<sub>3</sub><sup>-</sup>, NO<sub>2</sub><sup>-</sup>, NH<sub>4</sub><sup>+</sup>, PO<sub>4</sub><sup>3-</sup>) and chlorophyll a were collected from the  
inner Kubitzer Bodden (referred to in the following as “inner bay”) at station D1 (Figure 2a) and irregularly at a second station  
160 right in front of the now removed dike section, which was abandoned after rewetting and therefore merged with station D1.  
Environmental variables (water temperature, dissolved oxygen (O<sub>2</sub>), salinity) were measured on-site. Both stations were  
reached from land and sampling was conducted monthly from June to November 2019, except in August.

After rewetting, surface water samples were collected with a small boat and the sampled variables were extended for  
the concentrations of GHGs (CO<sub>2</sub>, CH<sub>4</sub>, N<sub>2</sub>O) and dissolved organic carbon (DOC). The first sampling took place one week  
165 after the dike removal. Sampling was continued over one year (25 sampling dates until December 2020) at weekly (December  
2019 to January 2020) or biweekly (February 2020 to September 2020, except for August) intervals. From October 2020 to  
December 2020, sampling was conducted monthly. In the inner bay, three stations (D1, D3, D14), and in the flooded peatland  
six stations (D4, D5, D11, D12, D15, BTD8) were sampled (Figure 2a). The inner bay station “D14” was sampled from March

2020 onwards. DOC sampling started in April 2020. For the air-sea gas exchange calculation, data from station D10\_1, located  
170 in the channel, were also included.

Moreover, surface water samples for the analysis of GHG concentrations ( $\text{CO}_2$ ,  $\text{CH}_4$ ,  $\text{N}_2\text{O}$ ) were sampled at eight stations along a transect (Figure 2b). This sampling was carried out simultaneously with the sampling described in Sect. 2.2.2 to link GHG air-sea exchange calculations based on surface water samples with chamber-based flux measurements.

Surface water temperature,  $\text{O}_2$ , and salinity were measured directly in the field using a HACH HQ40D multimeter  
175 (HACH Lange GmbH, Germany) equipped with two outdoor electrodes (LDO10105, CDC40105). Depending on the prevailing water depth, additional measurements were conducted in the peatland 15 cm above the soil surface (excluding the ditches) on 22 of the 25 sampling dates. The precision of the electrodes was  $\pm 0.3$  °C,  $\pm 0.8$  %, and  $\pm 0.1$  for temperature,  $\text{O}_2$  saturation, and salinity, respectively.

Surface water samples were taken using a horizontal 7 L Niskin bottle to sample the upper 20 cm of the water column.  
180 These included 250 mL subsamples for  $\text{CH}_4/\text{N}_2\text{O}$  analysis (bottles capped with butyl rubber stoppers and crimp-sealed), analysis of the  $\text{CO}_2$  system (one bottle each for total  $\text{CO}_2$  ( $C_T$ ), total alkalinity ( $A_T$ ), and pH) and 15 mL subsamples for the analysis of nutrients and DOC. Water for chlorophyll a determination was taken using 3 L canisters.

In the laboratory,  $\text{CH}_4/\text{N}_2\text{O}$  and  $\text{CO}_2$  samples were poisoned with 500  $\mu\text{L}$  and 200  $\mu\text{L}$  of saturated  $\text{HgCl}_2$ , respectively, and stored in the dark at 4°C until analysis. Subsamples for nutrients and DOC were filtered in the field with pre-combusted  
185 (450 °C for 4 h) 0.7  $\mu\text{m}$  glass-fiber filters (GF/F, Whatman®) and stored at -20 °C. Samples for chlorophyll a were filtered in the laboratory with non-combusted 0.7  $\mu\text{m}$  glass-fiber filters (GF/F, Whatman®) and likewise stored at -20 °C.

### 2.2.2 Chamber-based atmospheric GHG flux sampling for $\text{CO}_2$ and $\text{CH}_4$

Starting in June 2019, nearly 6 months before rewetting, GHG exchange was regularly measured using dynamic closed chambers (Livingston and Hutchinson, 1995) along a transect representing a soil humidity gradient (Figure 2b). The  
190 measurements were conducted twice a month, for a total of eleven sampling days at six peatland stations and two additional stations in the north-south-oriented main ditch. Each station was sampled up to eight times per sampling day, resulting in overall 418  $\text{CO}_2$  and 184  $\text{CH}_4$  pre-rewetting flux measurements.

For each measurement, the chambers were placed on permanently installed collars and connected through an air-tight seal, with a closure period between 180 and 300 s. Between the measurements, chambers were lifted to vent them until  
195 atmospheric GHG concentrations were reached. To ensure coverage of photosynthetic and respiration activity,  $\text{CO}_2$  measurements on the terrestrial peatland were conducted using opaque and transparent chambers for NEE (net ecosystem exchange) and Reco (ecosystem respiration) determination, respectively. To cover a broad spectrum of solar radiation, two additional measurements were conducted with cloth-covered transparent chambers, resulting in a reduced photosynthetically active photon flux density (PPFD). Ditch stations' GHG concentrations were determined in three consecutive measurements  
200 with floating opaque chambers placed on the water surface. Changes in GHG concentrations in the chamber headspace were measured using a portable laser-based analyzer (Picarro G4301, GasScouter, Santa Clara, USA; LI-820, LI-COR Biosciences,

Lincoln, USA and an Ultraportable Greenhouse Gas Analyzer (UGGA), Los Gatos Research Inc., Mountain View, Calif., USA).

205 After rewetting, the stations along the transect covered a gradient of ground elevations, including stations that fell dry at low water levels and stations that remained permanently flooded. Atmospheric GHG fluxes were measured twice a month using floating opaque chambers positioned above the same sampling locations of the flooded peatland. Since the flooding caused most plants to die, and almost all measurement locations were covered by water during the study period, we reduced the number of NEE measurements with transparent chambers to stations and days with low water table. Approximately six measurements per station were made during 23 sampling days between December 2019 and December 2020, with a total of 210 698 CO<sub>2</sub> and 482 CH<sub>4</sub> fluxes determined during the post-rewetting year.

### 2.3 Data processing, statistics, and definition of seasons and means

Data analysis and visualization were performed using R (R Core Team, 2020) and the packages *tidyverse* (Wickham et al., 2019), *lubridate* (Grolemund and Wickham, 2011), *patchwork* (Pedersen, 2020) *car* (Fox and Weisberg, 2019), and *flux* (Jurasinski et al., 2014). The relationships between environmental variables, nutrient concentrations, and GHG 215 concentrations/fluxes were investigated in linear regression analyses. The significance level was set to  $p < 0.05$ .

To describe temporal patterns during the entire sampling period, we defined two pre- and four post-rewetting periods, roughly corresponding to seasons (Table 1). For a direct comparison between the pre- and post-rewetting periods, we compared nutrient and GHG flux data from summer and autumn 2019 with those from summer and autumn 2020 (Table 3) by using the Mann-Whitney-U test.

220 **Table 1.** Defined seasons of the investigation period

	Pre-rewetting		Post-rewetting			
season	summer 2019	autumn 2019	winter 2019/2020	spring 2020	summer 2020	autumn 2020
months	June–August	September–November	December–February	March–May	June–August	September–December

We analyzed the data among the respective peatland and inner bay stations in order to verify the use of means for each sampling site (peatland and inner bay separately) and date. The difference between spatial (sampling stations of either sites) and temporal (sampling seasons) data variability was tested by using a Two-Way ANOVA and showed a higher temporal variability 225 ( $p < 0.05$ ). Therefore, we decided to combine the stations within the peatland and within the inner bay, respectively, to report mean values and standard deviations (single values can be found in the published data set). The Two-Way ANOVA was also used to identify seasonal differences between the peatland and the inner bay (Table 2).

At station D3, in the inner bay, the pH, CH<sub>4</sub>, and pCO<sub>2</sub> values differed significantly from those of the remaining stations of the inner bay during the year after rewetting (ANOVA, Kruskal-Wallis test). Since the differences in water 230 temperature, salinity, and O<sub>2</sub> were not significant, we decided to include the data from D3 for these variables to obtain a larger data pool for the inner bay and to exclude D3 for all other variables. The exclusion was conducted because variables such as



pH, CH<sub>4</sub>, and pCO<sub>2</sub> are related to biological activity which can vary, while the more physically influenced variables (temperature, salinity, and O<sub>2</sub>) are rather constant.

## **2.4 Nutrients (NO<sub>3</sub><sup>-</sup>, NO<sub>2</sub><sup>-</sup>, NH<sub>4</sub><sup>+</sup>, PO<sub>4</sub><sup>3-</sup>), chlorophyll a and DOC**

### 235 **2.4.1 Analysis**

Nutrient analyses were carried out according to standard photometric methods (Grasshoff et al., 2009) by using a continuous segmented flow analyzer (SEAL Analytical QuAAtro, SEAL Analytical GmbH, Norderstedt, Germany). Detection limits were 0.2 μM for NO<sub>3</sub><sup>-</sup>, 0.05 μM for NO<sub>2</sub><sup>-</sup>, 0.5 μM for NH<sub>4</sub><sup>+</sup> and 0.1 μM for PO<sub>4</sub><sup>3-</sup>. Measurements of the nutrient concentrations were partly below the detection limit for the peatland, the inner bay and the central bay (flagged in the published dataset). For  
240 such measurements below detection limit, it is recommended to use the actual values of these measurements (e.g. Fiedler et al., 2022) to achieve a robust statistical analysis. Since these data were not available, we decided to use randomly generated values between 0 and the respective detection limit with a uniform distribution for these measurements.

Chlorophyll a was extracted from glass-fiber filters (GF/F, Whatman<sup>®</sup>) by incubation with 96 % ethanol for 3 h and afterwards analyzed by using a fluorometer (TURNER 10-AU-005, Turner Designs, San José, USA) at 670 nm according to  
245 Edler (1979). DOC was analyzed after high-temperature combustion using a Multi 2100S instrument (Analytik Jena GmbH, Jena, Germany) and detected by non-dispersive infrared spectrometry according to ISO 20236, ISO 8245 I, and EN 1484.

### **2.4.2 Use of reference data from a monitoring station**

Coastal nutrient data (NO<sub>3</sub><sup>-</sup>, NO<sub>2</sub><sup>-</sup>, NH<sub>4</sub><sup>+</sup> and PO<sub>4</sub><sup>3-</sup> concentrations) from a monitoring station in the Kubitzer Bodden (“central bay”, Figure 1b) ~15 km away from the study area were obtained as reference. Monitoring data from 2016 to 2020 were  
250 included. These data were used (1) to compare them with nutrient concentrations from the inner bay before and after rewetting to detect potentially higher concentrations, resulting from nutrient leaching within the peatland and a subsequent export into the inner bay and (2) to calculate the total possible export out of the peatland (Sect. 2.4.3) by using the monitoring station as a second, unaffected endmember besides the inner bay, which is by contrast potentially affected by the rewetting. Due to transformations and potential losses along the way to the monitoring station, especially of the nitrogen species, the calculated  
255 total possible exports have to be considered as maximum estimates.

### **2.4.3 Nutrient transport calculation (DIN-N and PO<sub>4</sub>-P)**

To calculate the bulk exchanges of dissolved inorganic nitrogen (DIN-N) and PO<sub>4</sub>-P between the flooded peatland and the inner bay/central bay, the water level was transformed to water volume by creating a hypsographic curve with increments of 0.1 m and a resolution of 1x1 m (Figure A3). Water level data from a nearby monitoring station (“Barhöft”, 54.43° N, 13.03° E)  
260 and topography data with a resolution of 1x1 m were obtained from the Wasserstraßen- und Schifffahrtsamt Ostsee (WSA) and the Landesamt für innere Verwaltung MV, respectively. To ensure that the water level data of the monitoring station were

valid for the peatland, the water level data of the latter, measured between August and December 2020, were compared with the data from the monitoring station, which showed a strong correlation ( $r_s = 0.95$ ,  $p < 0.001$ , 15-min intervals, data not shown).

265 A water level of  $-1.6$  masl, as the lowest recorded water level within the last 25 years, was used as the starting point to derive the cumulative water volumes of the peatland. The water volumes were then assigned to the corresponding water levels to finally calculate the water volume changes ( $Q$ , in  $\text{m}^3 \text{s}^{-1}$ ) according to Eq. (1):

$$Q(t) = \frac{dV}{dt} \quad (1)$$

where  $V$  is the water volume and  $t$  the time. Positive volume changes ( $Q > 0$ ) indicate an inflow of water into the peatland and *vice versa*. For each season, the mean inflow ( $Q_{in}$ ) and outflow ( $Q_{out}$ ) volumes were calculated according to Eqs. (2) and (3):

$$Q_{in} = \frac{1}{\Delta T} \int_t^{t+\Delta T} Q^{positive} dt \quad \text{for } Q > 0 \quad (2)$$

$$Q_{out} = \frac{1}{\Delta T} \int_t^{t+\Delta T} Q^{negative} dt \quad \text{for } Q < 0 \quad (3)$$

270 where  $\Delta T$  denotes the season length. Note that  $Q_{out}$  is negative. Seasonal mean values of nutrient concentrations ( $\text{DIN}$  and  $\text{PO}_4^{3-}$ ) were calculated and converted from  $\mu\text{M}$  to  $\text{kg m}^{-3}$  by using the molecular masses of the basic elements  $\text{N}$  and  $\text{P}$  to derive  $\text{DIN-N}$  and  $\text{PO}_4\text{-P}$ . After the conversion, nutrient masses of the peatland ( $c_{peatland}$ ) and the inner bay ( $c_{IB}$ ) vs. peatland and central bay ( $c_{CB}$ ), respectively, were multiplied by  $Q_{out}$  and  $Q_{in}$  and integrated to calculate the net nutrient transport (NNT, in tonnes, equivalent to megagrams) according to Eqs. (4) and (5):

$$NNT = \int_t^{t+\Delta T} Q_{in} c_{IB} dt + \int_t^{t+\Delta T} Q_{out} c_{peatland} dt \quad (4)$$

$$NNT = \int_t^{t+\Delta T} Q_{in} c_{CB} dt + \int_t^{t+\Delta T} Q_{out} c_{peatland} dt \quad (5)$$

275 Negative values indicate a net nutrient export from the peatland into the inner/central bay, and positive values display a net nutrient import into the peatland. Uncertainty ranges for the seasonal NNTs ( $u_{NNT}$ , as 95 % confidence level) were calculated by using an error propagation according to Eq. (6):

$$u_{NNT} = \sqrt{(c_{bay} dt u_{Q_{in}})^2 + (c_{peat} dt u_{Q_{out}})^2 + (Q_{out} dt u_{c_{peat}})^2 + (Q_{in} dt u_{c_{bay}})^2} \quad (6)$$

where terms with “ $u$ ” denote the respective 95 % confidence level. To derive the annual uncertainty range of the NNT, all seasonal errors were added up.

## 280 2.5 GHG concentrations and fluxes

### 2.5.1 Inorganic carbon system analysis

#### Directly measured variables ( $C_T$ , $A_T$ , $\text{pH}$ )

The inorganic carbon system was determined by analyzing the total CO<sub>2</sub> (C<sub>T</sub>), total alkalinity (A<sub>T</sub>), and pH of the water samples. C<sub>T</sub> was measured with an automated infrared inorganic carbon analyzer (AIRICA, S/N #027, Marianda, Kiel, Germany). The system acidifies a discrete sample volume (phosphoric acid, 10 %), whereby the inorganic carbon species of C<sub>T</sub> are shifted to CO<sub>2(g)</sub>. A carrier gas stream (99.999 % N<sub>2</sub>) transfers the gaseous components to a Peltier device and a Nafion® drying tube (Perma Pure Nafion®, Ansyco GmbH, Karlsruhe, Germany) to remove water residues. The produced CO<sub>2(g)</sub> is detected by an infrared detector (LICOR 7000; LI-COR Environmental GmbH, Bad Homburg, Germany). Certified reference materials (CRM; Scripps Institution of Oceanography, University of California, San Diego, USA) were used for calibration. Triplicate measurements were conducted for each sample, and a precision of ± 5 μmol kg<sup>-1</sup> was achieved.

A<sub>T</sub> was measured by potentiometric titration (glass electrode type LL Electrode plus 6.0262.100, Metrohm, Filderstadt, Germany) in the open-cell configuration, after Dickson et al. (2007). The system was calibrated with the same CRM as used for C<sub>T</sub> and resulted in the same precision.

The pH was analyzed spectrophotometrically using the pH-sensitive indicator dye m-cresol purple (mCP, 2 mM, Contros System and Solution GmbH, Kiel, Germany). The measurement principle and instrumental setup are described elsewhere (Dickson et al., 2007; Carter et al., 2013). In brief, absorption was measured using the Agilent 8453 UV-visible spectroscopy system (Agilent Technology, Waldbronn, Germany); pH parameterization for brackish water was calculated following Müller and Rehder (2018). Quality control was performed by measuring buffer solutions (salinity of 20) prepared according to Müller et al. (2018). An external buffer solution with a salinity of 35 (Scripps Institution of Oceanography, University of California, San Diego, USA) was additionally used. All pH values are reported given on the total scale (pH<sub>T</sub>).

### Calculated variables

The CO<sub>2</sub> partial pressure in the water phase (pCO<sub>2</sub>), the value of which was required for the CO<sub>2</sub> air-water flux calculations (Sect. 2.5.3), was calculated from C<sub>T</sub> and pH using the R packages *seacarb* (Gattuso et al., 2019), with K<sub>1</sub> and K<sub>2</sub> from Millero (2010), K<sub>s</sub> from Dickson (1990), and K<sub>f</sub> from Dickson and Riley (1979). C<sub>T</sub> and pH were preferred because non-oceanic components, in particularly organic acid-base systems, contribute significantly to A<sub>T</sub> (Kuliński et al., 2014). A<sub>T</sub> was also calculated from C<sub>T</sub> and pH and the values compared with measured values, thus revealing the magnitude of the contributions of those components to A<sub>T</sub>.

### 2.5.2 Dissolved CH<sub>4</sub> and N<sub>2</sub>O concentration analysis

Dissolved CH<sub>4</sub> and N<sub>2</sub>O concentrations were determined by gas chromatography on an Agilent 7890B instrument (Agilent Technologies, Santa Clara, USA) coupled to a flame ionization detector (FID) and an electron capture detector (ECD). A purge and trap technique, explained in detail in Sabbaghzadeh et al. (2021) was used. In brief, a helium gas stream was used to purge 10 mL of seawater to extract volatile compounds. The gas stream passed through a purifier (VICI Valco Instruments Co. Inc., Houston, USA) and was dried using a Nafion® tube (Perma Pure Nafion®, Ansyco GmbH, Karlsruhe, Germany) and a SICAPENT® tube (Merck KGaA, Darmstadt, Germany). The relevant compounds were enriched by cryofocusing on a trap filled with HayeSep D® (CS Chromatographie Service GmbH, Langerwehe, Germany) maintained at -120 °C using an

ethanol/nitrogen cooling bath. After 10 minutes of heating in a 95 °C water bath, the compounds were desorbed and separated by two capillary columns linked to the detectors by a Deans Switch (Pönisch, 2018).

For quality control, a calibration standard (gas composition:  $9.9379 \pm 0.0159$  ppm CH<sub>4</sub> and  $1982.07 \pm 3.77$  ppb N<sub>2</sub>O) was measured daily before and after the sample measurements; the standard deviation was < 1 %. The calibration range was adjusted using multi-loop injection of the calibration gas to ensure that the samples were within the limits of the calibration. The standard was recalibrated according to high-precision standards (ICOS-CAL laboratory, Max Planck Institute, Jena, Germany).

### 2.5.3 GHG flux calculations

#### Atmospheric fluxes based on closed-chamber measurements

CO<sub>2</sub> and CH<sub>4</sub> fluxes were calculated using the ideal gas law (Livingston and Hutchinson, 1995), as formulated in Eq. (7):

$$F = \frac{MpV}{RTA} * \frac{dc}{dt} \quad (7)$$

where F is the GHG flux ( $\text{g m}^{-2} \text{h}^{-1}$ ), M is the molar mass of the gas ( $\text{g mol}^{-1}$ ), p is the standard air pressure (101,300 Pa), V is the chamber volume ( $\text{m}^3$ ), R is the gas constant ( $\text{m}^3 \text{Pa K}^{-1} \text{mol}^{-1}$ ), T is the temperature in the chamber (K), A is the surface area of the measurement collar ( $\text{m}^2$ ), and  $dc/dt$  is the change in concentration over time. The latter was derived from the slope of a linear regression based on the medians of the gas concentrations. The atmospheric sign convention was applied; thus, positive fluxes indicated a release of GHG by the soil and negative fluxes GHG uptake by the soil. The fluxes were estimated using the function *fluxx()* of the R package *flux* (Jurasinski et al., 2014) and the SLP method. Outlier identification (using a histogram) resulted in the exclusion of CO<sub>2</sub> fluxes which were smaller than  $-2.5$  and larger than  $4 \text{ g m}^{-2} \text{h}^{-1}$ . Likewise, CH<sub>4</sub> fluxes larger than  $200 \text{ mg m}^{-2} \text{h}^{-1}$  were discarded due to a high risk of capturing ebullition-based CH<sub>4</sub> emissions instead of diffusive fluxes.

335

#### Atmospheric fluxes based on air-sea gas exchange parameterization (velocity k model)

The air-sea gas exchange ( $F$ ,  $\text{g m}^{-2} \text{h}^{-1}$ ) is a function of the gas transfer velocity ( $k$ ) and the concentration difference between the bulk liquid ( $C_w$ ) and the top of the liquid boundary layer adjacent to the atmosphere ( $C_a$ ). It was calculated as reported in Wanninkhof (2014) and as shown in Eq. (8):

$$F = k (C_w - C_a) \quad (8)$$

where  $k$  was derived from an empirical relationship between a coefficient of gas transfer (0.251) and the wind speed  $\langle U^2 \rangle$  (Wanninkhof, 2014) and Schmidt number ( $Sc$ ), as expressed by Eq. (9):

$$k = 0.251 \langle U^2 \rangle (Sc/660)^{(-0.5)} \quad (9)$$

Wind speeds originated from the nearby (~15 km away) monitoring station Putbus and were measured at 10 m height (DWD; 54.3643° N, 13.4771° E, WMO-ID 10093). The average wind speed was defined in this study  $\pm 3$  h from midday, because the wind speed over 24 h was lowest at night and highest at midday and because sampling was usually conducted within the

345 selected time interval. The Schmidt number was approximated by a linear interpolation between the freshwater and seawater values. Atmospheric-equilibrium conditions ( $C_a$ ) were calculated using the atmospheric data for  $\text{CO}_2$  and  $\text{CH}_4$  obtained from the ICOS station “Utö” (Finnish Meteorological Institute, Helsinki). Due to the seasonal changes in the atmospheric dry molar fraction of  $\text{CO}_2$  and  $\text{CH}_4$ , mean values for each season were computed. For  $\text{N}_2\text{O}$ , the atmospheric dry mole fraction from station Mace Head was selected (National University of Ireland, Galway; data from the NOAA GML carbon cycle cooperative global  
350 air sampling network (Dlugokencky et al., 2019a, 2019b)). A mean value of the atmospheric  $\text{N}_2\text{O}$  concentration during the investigation period was calculated due to its minor seasonality. Equilibrium concentrations were then calculated using the solubility coefficient ( $K_0$ ) from Weiss and Price (1980). We acknowledge that the air-sea exchange model we used (Wanninkhof, 2014) was developed for open ocean waters and is a doubtful approach for deriving fluxes in small enclosed areas such as our working area. However, the lack of an appropriate parameterization, and the convincing result of the  
355 comparison of our two approaches (see below and Appendix C: Comparability of two independent approaches to atmospheric flux determination) justify our approach.

### **Comparability of two independent approaches to atmospheric flux determination**

We evaluated the comparability of the two previously described methods by comparing the results of a representative station (BTD7) for each post-rewetting season. The comparison showed no significant differences between the fluxes of  $\text{CO}_2$  and  $\text{CH}_4$   
360 derived with the different methods and therefore, it seems appropriate to combine the fluxes for each GHG into one pooled post-rewetting data set. The pooled post-rewetting flux values were compared with the pre-rewetting values to investigate the effect of rewetting on  $\text{CH}_4$  and  $\text{CO}_2$  fluxes (Table 3). For more details concerning the comparability assessment, see Appendix C: Comparability of two independent approaches to atmospheric flux determination. Due to the large variability and the pooling of chamber-based measurements with k model data, the GHG fluxes after rewetting are hardly suitable for upscaling  
365 and thus, the single values in the published data should be used.

## **3. Results**

### **3.1 Surface water properties (temperature, salinity, $\text{O}_2$ , DOC, chlorophyll a)**

In the first year after rewetting, there were no significant differences between the peatland and the inner bay with respect to surface water temperature, salinity and  $\text{O}_2$  saturation (Figure 3a–c, Table 2), suggesting a pronounced water exchange between  
370 the peatland and the inner bay that was driven by frequent changes in the water level (Figure A1). Additionally, no significant differences between summer and autumn 2019 and summer and autumn 2020 were found in the inner bay.

Temperature and salinity measurements near the peat surface showed no significant differences between the surface and bottom water over the year ( $n_{\text{surface}} = 140$ ,  $n_{\text{bottom}} = 86$ , data not shown), which suggested that vertical exchange processes and mixing were highly pronounced. However, a significant difference in  $\text{O}_2$  saturation between the surface and bottom water  
375 in summer ( $p < 0.01$ ) indicated that local and temporary gradients are possible.

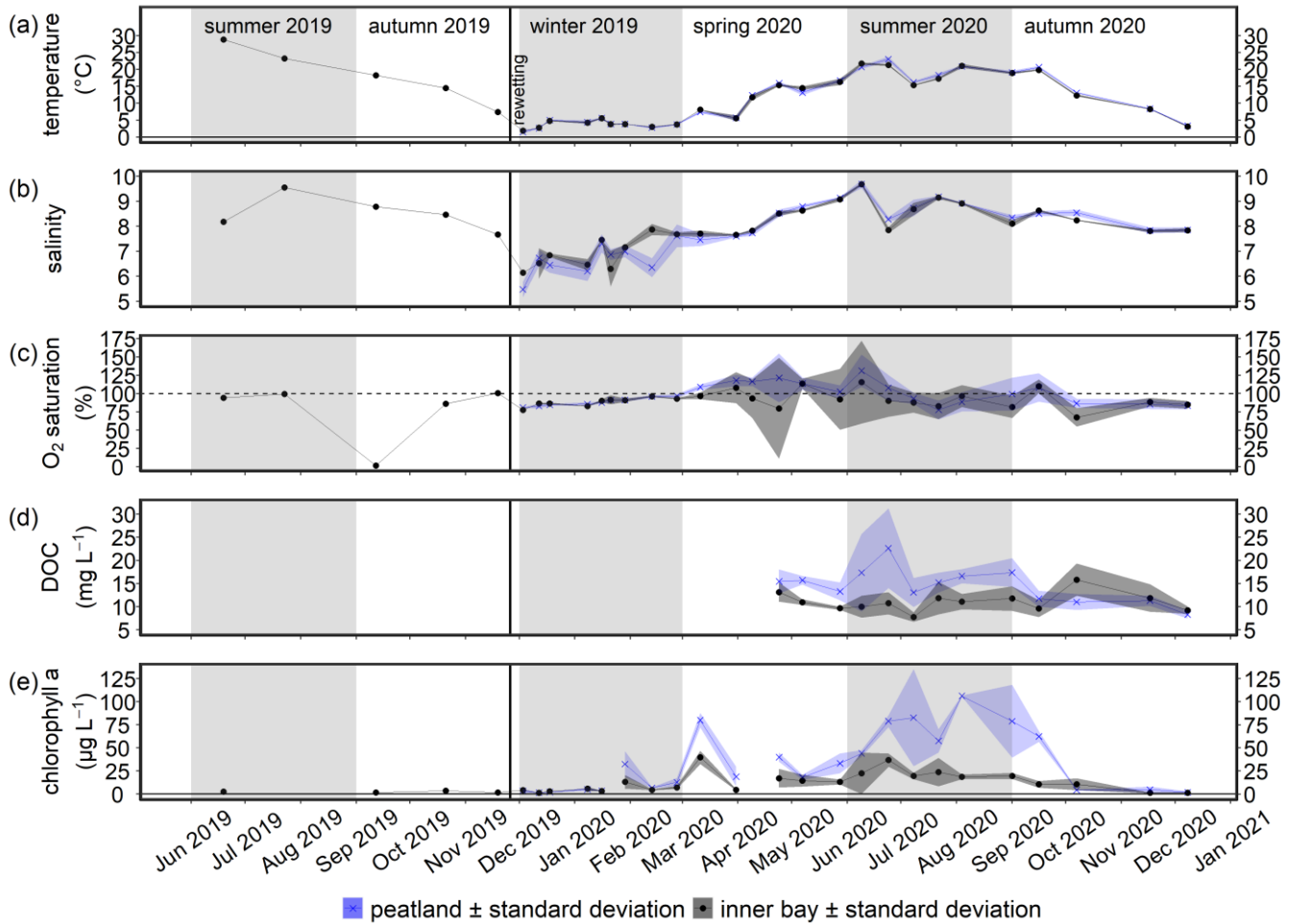


**Figure 3.** Time series of the mean (a) temperature, (b) salinity, (c) O<sub>2</sub> saturation, (d) DOC concentration and (e) chlorophyll a concentration ( $\pm$  standard deviations) in the surface water from June 2019 to December 2020. Data from the flooded peatland ( $n = 6$ ) are shown in blue and data from the inner bay ( $n = 2$  or  $3$ , as explained in Sect. 2.3) in black. The vertical black line indicates the rewetting event.

380 DOC concentrations were significantly higher in the peatland than in the inner bay in spring and summer, with the highest concentration ( $\sim 30 \text{ mg L}^{-1}$ ) measured in the peatland (Figure 3d, Table 2). Chlorophyll a concentrations after rewetting showed clear seasonal and spatial differences, with significantly higher concentrations in the peatland in spring and summer (max.  $\sim 125 \text{ } \mu\text{g L}^{-1}$ , Figure 3e, Table 2). A comparison of pre- and post-rewetting chlorophyll a concentrations in the inner bay in summer and autumn showed higher concentrations after rewetting (pre-rewetting:  $2.5 \pm 0.9 \text{ } \mu\text{g L}^{-1}$ , post-rewetting: 385  $15.4 \pm 11.5 \text{ } \mu\text{g L}^{-1}$ ).

**Table 2.** Seasonal comparison of the surface water means ( $\pm$  standard deviation) in the peatland (“peat”) as opposed to the inner bay (“bay”) for all in situ variables. The number of observations is shown in parentheses, and significant seasonal differences ( $p < 0.05$ ) between the inner bay and the peatland are indicated in bold.

		Pre-rewetting		Post-rewetting			
		summer 2019	autumn 2019	winter 2019	spring 2020	summer 2020	autumn 2020
temperature (°C)	peat	N/A	N/A	3.73 $\pm$ 1.25 (45)	12.03 $\pm$ 4.17 (35)	19.85 $\pm$ 2.44 (30)	12.94 $\pm$ 6.61 (30)
	bay	25.17 $\pm$ 3.27 (3)	13.95 $\pm$ 3.59 (6)	3.86 $\pm$ 0.99 (17)	12.17 $\pm$ 4.09 (17)	19.36 $\pm$ 2.68 (15)	12.52 $\pm$ 6.58 (15)
salinity	peat	N/A	N/A	6.67 $\pm$ 0.68 (45)	8.23 $\pm$ 0.66 (35)	8.96 $\pm$ 0.50 (30)	8.22 $\pm$ 0.33 (30)
	bay	9.21 $\pm$ 0.69 (4)	8.39 $\pm$ 0.38 (6)	6.99 $\pm$ 0.65 (17)	8.27 $\pm$ 0.56 (17)	8.86 $\pm$ 0.63 (15)	8.13 $\pm$ 0.32 (15)
O <sub>2</sub> (mg L <sup>-1</sup> )	peat	N/A	N/A	11.19 $\pm$ 0.74 (45)	11.72 $\pm$ 1.93 (35)	8.60 $\pm$ 1.86 (30)	9.34 $\pm$ 1.35 (30)
	bay	7.66 $\pm$ 1.70 (3)	7.48 $\pm$ 3.87 (6)	11.18 $\pm$ 0.67 (17)	10.03 $\pm$ 3.48 (17)	8.26 $\pm$ 2.26 (15)	8.86 $\pm$ 1.80 (15)
chlorophyll a (µg L <sup>-1</sup> )	peat	N/A	N/A	8.55 $\pm$ 10.80 (24)	<b>40.03 <math>\pm</math> 26.39 (12)</b>	<b>74.03 <math>\pm</math> 29.01 (10)</b>	30.57 $\pm$ 37.50 (10)
	bay	2.66 $\pm$ N/A (1)	2.42 $\pm$ 1.09 (3)	4.76 $\pm$ 2.31 (8)	<b>13.52 <math>\pm</math> 8.90 (8)</b>	<b>21.91 <math>\pm</math> 11.04 (10)</b>	8.83 $\pm$ 7.76 (10)
DOC (mg L <sup>-1</sup> )	peat	N/A	N/A	N/A	<b>14.82 <math>\pm</math> 2.13 (18)</b>	<b>16.95 <math>\pm</math> 6.09 (27)</b>	12.07 $\pm$ 3.47 (29)
	bay	N/A	N/A	N/A	<b>11.78 <math>\pm</math> 2.12 (6)</b>	<b>10.72 <math>\pm</math> 2.73 (10)</b>	11.09 $\pm$ 2.54 (10)
NO <sub>3</sub> <sup>-</sup> (µM)	peat	N/A	N/A	100.03 $\pm$ 57.66 (45)	25.22 $\pm$ 46.03 (35)	0.14 $\pm$ 0.10 (29)	3.69 $\pm$ 3.99 (30)
	bay	0.36 $\pm$ 0.30 (4)	2.33 $\pm$ 2.80 (6)	68.50 $\pm$ 40.67 (9)	15.38 $\pm$ 30.68 (11)	0.16 $\pm$ 0.12 (10)	3.38 $\pm$ 3.56 (10)
NO <sub>2</sub> <sup>-</sup> (µM)	peat	N/A	N/A	<b>1.49 <math>\pm</math> 0.62 (45)</b>	0.43 $\pm$ 0.44 (35)	0.23 $\pm$ 0.12 (29)	0.99 $\pm$ 1.03 (30)
	bay	0.11 $\pm$ 0.07 (4)	0.19 $\pm$ 0.11 (6)	<b>1.04 <math>\pm</math> 0.49 (9)</b>	0.29 $\pm$ 0.33 (11)	0.16 $\pm$ 0.12 (10)	1.11 $\pm$ 1.20 (10)
NH <sub>4</sub> <sup>+</sup> (µM)	peat	N/A	N/A	30.02 $\pm$ 26.13 (45)	2.27 $\pm$ 1.56 (35)	5.54 $\pm$ 6.48 (29)	18.78 $\pm$ 19.50 (30)
	bay	1.67 $\pm$ 1.33 (3)	3.00 $\pm$ 1.70 (6)	21.47 $\pm$ 23.42 (9)	1.71 $\pm$ 1.13 (11)	2.82 $\pm$ 3.87 (10)	17.03 $\pm$ 21.78 (10)
PO <sub>4</sub> <sup>3-</sup> (µM)	peat	N/A	N/A	0.37 $\pm$ 0.41 (45)	<b>0.26 <math>\pm</math> 0.28 (35)</b>	<b>0.49 <math>\pm</math> 0.26 (29)</b>	0.35 $\pm$ 0.33 (30)
	bay	1.30 $\pm$ 1.90 (4)	0.12 $\pm$ 0.08 (6)	0.21 $\pm$ 0.21 (9)	<b>0.09 <math>\pm</math> 0.13 (11)</b>	<b>0.22 <math>\pm</math> 0.21 (10)</b>	0.26 $\pm$ 0.28 (10)
CH <sub>4</sub> (nmol L <sup>-1</sup> )	peat	N/A	N/A	47.96 $\pm$ 49.52 (46)	300.49 $\pm$ 414.29 (35)	<b>1502.36 <math>\pm</math> 693.36 (30)</b>	<b>733.74 <math>\pm</math> 699.17 (30)</b>
	bay	N/A	N/A	81.37 $\pm$ 106.93 (7)	130.12 $\pm$ 190.54 (11)	<b>502.47 <math>\pm</math> 479.31 (10)</b>	<b>194.70 <math>\pm</math> 186.49 (20)</b>
N <sub>2</sub> O (nmol L <sup>-1</sup> )	peat	N/A	N/A	85.53 $\pm$ 152.45 (46)	15.42 $\pm$ 4.97 (35)	<b>6.95 <math>\pm</math> 1.35 (30)</b>	14.34 $\pm$ 4.04 (30)
	bay	N/A	N/A	26.74 $\pm$ 9.69 (7)	13.13 $\pm$ 4.13 (11)	<b>8.76 <math>\pm</math> 1.26 (10)</b>	16.68 $\pm$ 5.27 (10)
pCO <sub>2</sub> (µatm)	peat	N/A	N/A	1403.89 $\pm$ 674.79 (46)	<b>925.64 <math>\pm</math> 868.56 (35)</b>	<b>4016.69 <math>\pm</math> 2120.03 (30)</b>	2197.11 $\pm$ 1771.41 (30)
	bay	N/A	N/A	1050.00 $\pm$ 552.68 (7)	<b>297.81 <math>\pm</math> 93.57 (11)</b>	<b>1161.74 <math>\pm</math> 1275.46 (10)</b>	1151.68 $\pm$ 968.31 (10)
pH	peat	N/A	N/A	7.66 $\pm$ 0.21 (46)	<b>8.01 <math>\pm</math> 0.33 (35)</b>	<b>7.35 <math>\pm</math> 0.34 (30)</b>	<b>7.60 <math>\pm</math> 0.32 (30)</b>
	bay	N/A	N/A	7.78 $\pm$ 0.20 (7)	<b>8.32 <math>\pm</math> 0.13 (11)</b>	<b>7.95 <math>\pm</math> 0.48 (10)</b>	<b>7.86 <math>\pm</math> 0.36 (10)</b>
C <sub>T</sub> (µmol kg <sup>-1</sup> )	peat	N/A	N/A	2153.61 $\pm$ 121.07 (46)	<b>2471.11 <math>\pm</math> 223.74 (35)</b>	<b>2539.09 <math>\pm</math> 225.34 (30)</b>	2273.41 $\pm$ 312.95 (30)
	bay	N/A	N/A	2113.87 $\pm$ 73.73 (7)	<b>2201.63 <math>\pm</math> 98.45 (11)</b>	<b>2094.51 <math>\pm</math> 208.11 (10)</b>	2106.76 $\pm$ 282.17 (10)
A <sub>T</sub> (µmol kg <sup>-1</sup> )	peat	N/A	N/A	2154.43 $\pm$ 155.12 (46)	<b>2614.86 <math>\pm</math> 209.57 (35)</b>	<b>2546.03 <math>\pm</math> 239.96 (30)</b>	2290.59 $\pm$ 272.70 (30)
	bay	N/A	N/A	2144.41 $\pm$ 94.49 (7)	<b>2414.45 <math>\pm</math> 123.87 (11)</b>	<b>2270.25 <math>\pm</math> 125.07 (10)</b>	2187.83 $\pm$ 213.75 (10)

**Table 3.** Statistical comparison of pre- and post-rewetting nutrient concentrations and GHG fluxes. For pre- and post-rewetting phases, summer and autumn seasons were used (June to November 2019 and 2020, respectively). Nutrient concentrations are compared for the inner bay and GHG fluxes for the peatland site. \*\*\* and "n.s." indicate  $p < 0.001$  and not significant, respectively.

	location	Pre-rewetting		Post-rewetting		<i>p</i>
		mean $\pm$ SD	n	mean $\pm$ SD	n	
NH <sub>4</sub> <sup>+</sup> ( $\mu$ M)	inner bay	2.6 $\pm$ 1.6	9	9.9 $\pm$ 16.9	20	n.s.
NO <sub>3</sub> <sup>-</sup> ( $\mu$ M)	inner bay	1.5 $\pm$ 2.3	10	1.8 $\pm$ 2.9	20	n.s.
NO <sub>2</sub> <sup>-</sup> ( $\mu$ M)	inner bay	0.2 $\pm$ 0.1	10	0.6 $\pm$ 1.0	20	n.s.
PO <sub>4</sub> <sup>3-</sup> ( $\mu$ M)	inner bay	0.6 $\pm$ 1.3	10	0.2 $\pm$ 0.2	20	n.s.
CO <sub>2</sub> flux (g m <sup>-2</sup> h <sup>-1</sup> )	transect + area	0.3 $\pm$ 0.8	330	0.3 $\pm$ 0.3	450	n.s.
CO <sub>2</sub> flux (g m <sup>-2</sup> h <sup>-1</sup> )	ditch	0.3 $\pm$ 0.1	87	0.3 $\pm$ 0.3	92	n.s.
CH <sub>4</sub> flux (mg m <sup>-2</sup> h <sup>-1</sup> )	transect + area	0.1 $\pm$ 1.0	97	1.7 $\pm$ 7.6	320	***
CH <sub>4</sub> flux (mg m <sup>-2</sup> h <sup>-1</sup> )	ditch	11.4 $\pm$ 37.5	85	8.5 $\pm$ 26.9	92	***

### 3.2 Nutrients (NO<sub>3</sub><sup>-</sup>, NO<sub>2</sub><sup>-</sup>, NH<sub>4</sub><sup>+</sup>, PO<sub>4</sub><sup>3-</sup>)

#### 395 3.2.1 Pre- and post-rewetting spatio-temporal dynamics and comparison with a nearby monitoring station

In the inner bay, all N-nutrient concentrations were substantially higher at the first sampling after rewetting than prior to rewetting, while PO<sub>4</sub><sup>3-</sup> concentrations were only slightly higher post-rewetting (Figure 4). This increase of N-nutrients led to a drastic increase of the N:P ratio from ~73 in autumn 2019 before rewetting to ~1600 shortly after rewetting in winter 2019. A comparison of the same pre- and post-rewetting seasons (summer and autumn 2019/2020) showed generally higher N-  
400 nutrient concentrations in the inner bay after rewetting which could not be confirmed statistically (Mann-Whitney-U-test, Table 3).

During winter, all N-nutrients were high in the peatland and inner bay. After a rapid decrease in spring, N-nutrient concentrations reached their lowest values during summer, with NH<sub>4</sub><sup>+</sup> and NO<sub>2</sub><sup>-</sup> then increasing in autumn again. PO<sub>4</sub><sup>3-</sup> concentrations followed a different pattern, with the highest concentrations determined in summer and fewer fluctuations over  
405 the year.

The spatial differences in nutrient concentrations between the inner bay and the peatland after rewetting varied greatly between the nutrient species. From the N-nutrients, only NO<sub>2</sub><sup>-</sup> concentrations were significantly higher once in winter, shortly after rewetting, whereas NH<sub>4</sub><sup>+</sup> and NO<sub>3</sub><sup>-</sup> concentrations showed no significant differences in any season (Table 2). Significantly higher PO<sub>4</sub><sup>3-</sup> concentrations in the peatland occurred during spring and summer ( $p < 0.05$ ). Some significant correlations  
410 between nutrient species were found (Figure D1), especially between NO<sub>2</sub><sup>-</sup>/NH<sub>4</sub><sup>+</sup> and NO<sub>3</sub><sup>-</sup>/NO<sub>2</sub><sup>-</sup> both in the peatland and the inner bay.

Nutrient concentrations of the monitoring station ("central bay") showed a low inter-annual variability during the years 2016–2020 and often lower concentrations than the inner bay (Figure 5). A detailed comparison of nutrient data from the monitoring station with those from the inner bay showed that before rewetting, only the NH<sub>4</sub><sup>+</sup> concentrations were



415 significantly higher in the inner bay. After rewetting,  $\text{NO}_3^-$  and  $\text{NO}_2^-$  concentrations in the inner bay increased and were significantly higher than in the central bay ( $p < 0.001$  and  $p < 0.05$ , respectively). In spring, N-nutrient concentrations were similar at the two locations whereas in summer, all N-nutrients were significantly higher in the inner bay ( $p < 0.01$ ). In autumn,  $\text{NO}_2^-$  and  $\text{NH}_4^+$  concentrations increased again and thus, showed significantly higher concentrations in the inner bay.  $\text{PO}_4^{3-}$  again followed a pattern different from that of the N-nutrients. Shortly before rewetting, its concentrations in the inner bay were significantly lower than those in the central bay ( $p < 0.05$ ). After rewetting,  $\text{PO}_4^{3-}$  concentrations showed no significant differences in any season.

420

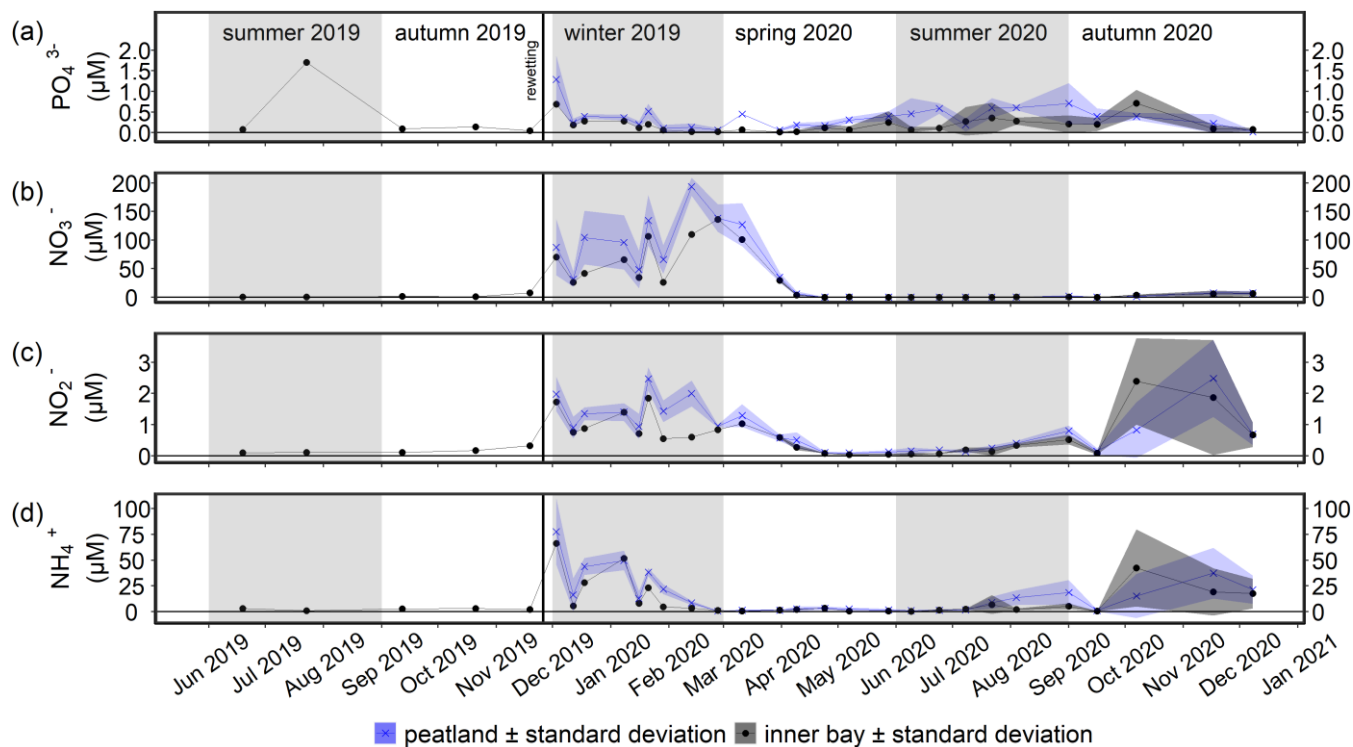


**Figure 4.** Time series of the mean (a)  $\text{PO}_4^{3-}$ , (b)  $\text{NO}_3^-$ , (c)  $\text{NO}_2^-$ , and (d)  $\text{NH}_4^+$  concentrations ( $\pm$  standard deviations) in the surface water from June 2019 to December 2020. Data from the flooded peatland ( $n = 6$ ) are shown in blue and data from the inner bay (until 11 March 2020:  $n = 1$ , thereafter:  $n = 2$ ) in black. The vertical black line indicates the rewetting event.

425

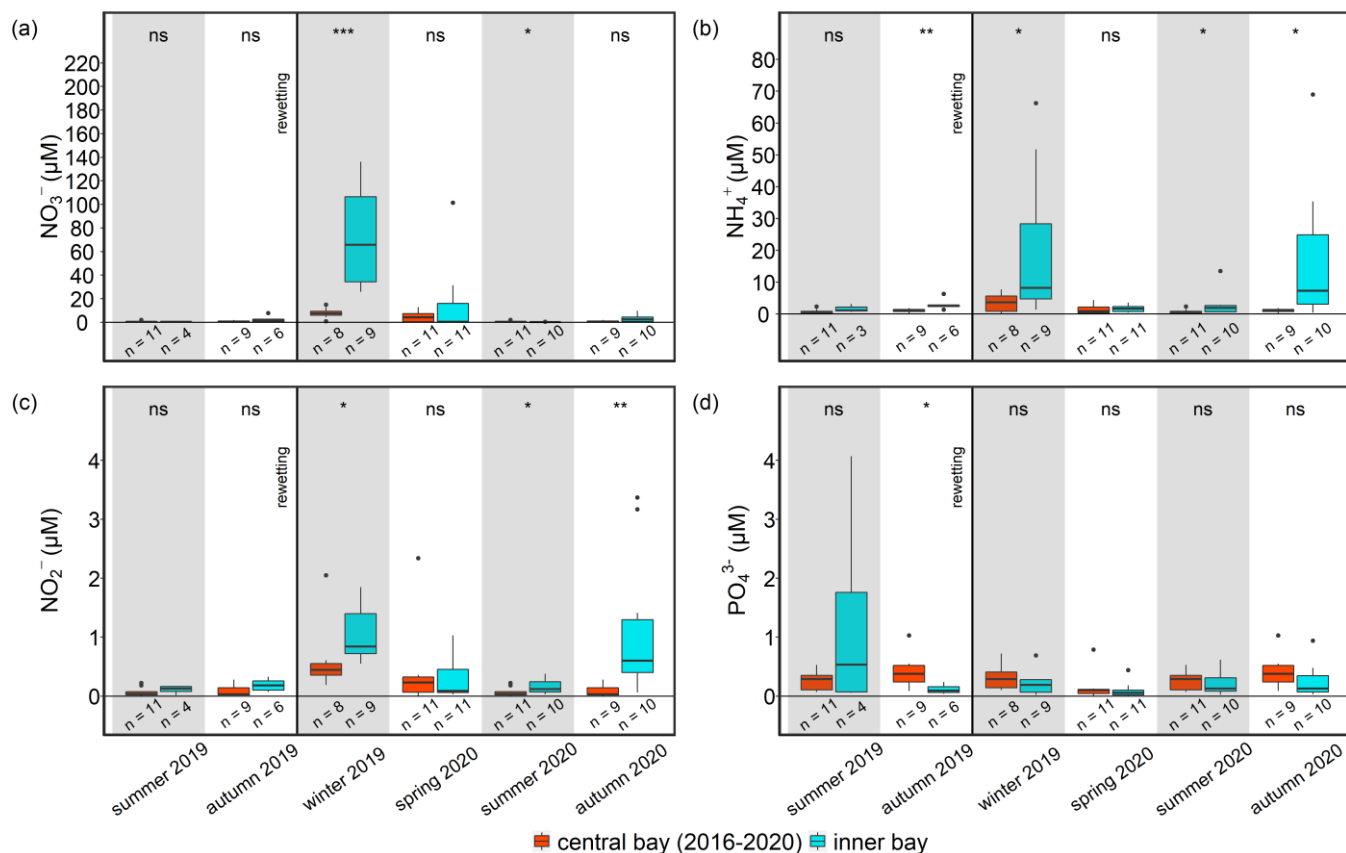


**Figure 5.** Seasonal nutrient concentrations of (a)  $\text{NO}_3^-$ , (b)  $\text{NH}_4^+$ , (c)  $\text{NO}_2^-$ , and (d)  $\text{PO}_4^{3-}$  at the nearby monitoring station (central bay, red) and in the inner bay (inner bay, blue) from pre- to post-rewetting. The vertical black line indicates the rewetting event. Note that 5-year-data (2016–2020) are shown for the central bay (see Sect. 2.4.2). ns = not significant, \* =  $p < 0.05$ , \*\* =  $p < 0.01$ , \*\*\* =  $p < 0.001$ .

### 3.2.2 Nutrient export from the rewetted peatland into the inner bay

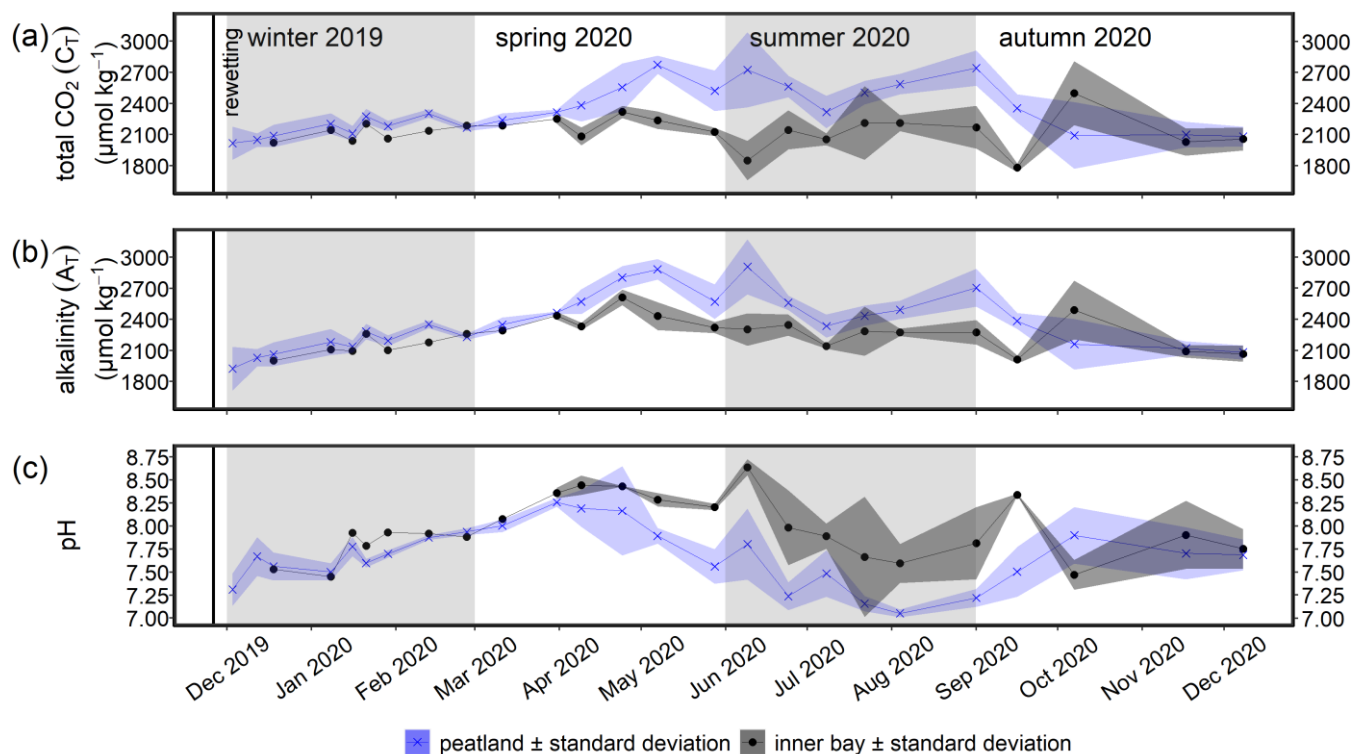
The rewetted peatland was a net source of DIN-N and  $\text{PO}_4\text{-P}$  for the inner bay (Table B1). During the first year after rewetting,  $10.8 \pm 17.4 \text{ t yr}^{-1}$  DIN-N and  $0.24 \pm 0.29 \text{ t yr}^{-1}$   $\text{PO}_4\text{-P}$  were exported into the inner bay (given as mean  $\pm$  95 % confidence level, equivalent to megagrams  $\text{yr}^{-1}$ ). DIN-N export was highest during the winter directly after rewetting ( $8.6 \pm 9.9 \text{ t}$ ) and lowest during summer ( $0.3 \pm 0.5 \text{ t}$ ). DIN-N and  $\text{PO}_4\text{-P}$  were only exported from the peatland into the inner bay in all seasons.

N-nutrient concentrations showed a gradient from the peatland through the inner bay to the central bay. Therefore, nutrient data from the central bay were also taken into account to estimate the total possible export from the peatland to the sea. This resulted in an estimated total net export of  $33.8 \pm 9.6 \text{ t yr}^{-1}$  DIN-N. In contrast to the comparison of the peatland and the inner bay,  $\text{PO}_4\text{-P}$  was once imported from the central bay into the peatland in autumn ( $0.03 \pm 0.10 \text{ t}$ ). Additionally, it was noticeable that the  $\text{PO}_4\text{-P}$  concentrations in the central bay were permanently higher than in the inner bay, leading to a lower annual export of  $0.09 \pm 0.32 \text{ t yr}^{-1}$   $\text{PO}_4\text{-P}$ .

### 3.3 GHG in the surface water after rewetting

#### 3.3.1 Inorganic C system

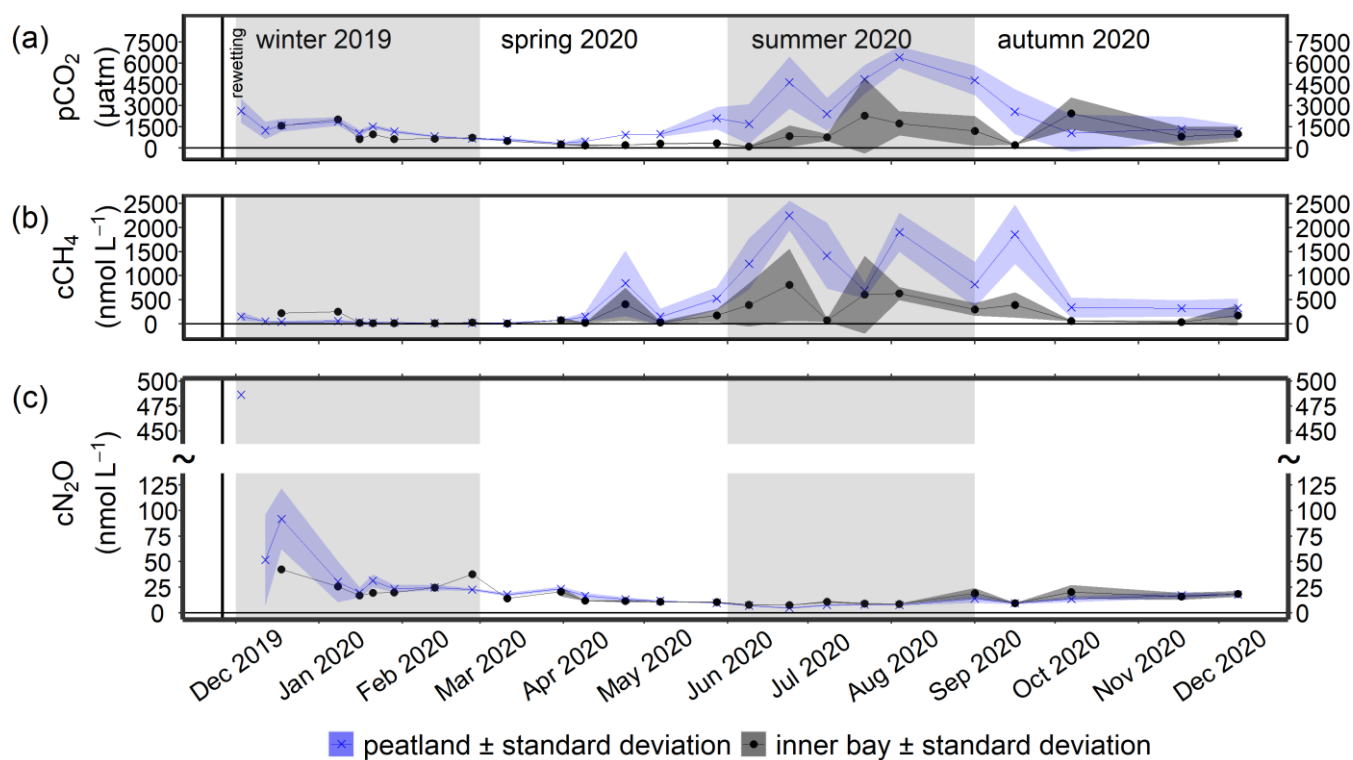
During the winter after rewetting, the differences in the CO<sub>2</sub> system (C<sub>T</sub>, A<sub>T</sub>, pH, pCO<sub>2</sub>) between the inner bay and the peatland were not significant (Figure 6, Figure 7a). All variables increased slightly until spring, coinciding with a slight increase in salinity over the same period. From spring onwards, however, the components of the CO<sub>2</sub> system followed contrasting patterns, with C<sub>T</sub> and A<sub>T</sub> remaining relatively constant in the inner bay but reaching significantly higher values in the peatland ( $p < 0.05$ ), including maximum values in summer (Table 2). The pH also showed significant seasonal differences, with lower values and a minimum in summer in the peatland ( $p < 0.05$ ). C<sub>T</sub> and A<sub>T</sub> values in the inner bay and in the peatland aligned in autumn whereas the pH remained significantly different ( $p < 0.05$ ). The mean pCO<sub>2</sub> (calculated from C<sub>T</sub> and pH) of the surface water in winter was  $1050.0 \pm 55.7 \mu\text{atm}$  in the inner bay and  $1403.9 \pm 674.8 \mu\text{atm}$  in the peatland (Figure 7a). The pCO<sub>2</sub> values were highest during the first few weeks after inundation and then steadily decreased, with the lowest mean values occurring in spring (peatland) and summer (inner bay). The summer was characterized by high pCO<sub>2</sub> values in general, including earlier and stronger increases in the peatland than in the inner bay that resulted in significant differences in spring and summer ( $p < 0.05$  for both seasons). pCO<sub>2</sub> values were highest in summer with  $4016.7 \pm 2120.0 \mu\text{atm}$  (peatland) and  $1161.7 \pm 1275.5 \mu\text{atm}$  (inner bay) (Table 2). In October, all of the examined CO<sub>2</sub> quantities had a short-term inversion of the prevailing pattern.



460 **Figure 6.** Time series of the mean (a) total CO<sub>2</sub> (C<sub>T</sub>), (b) total alkalinity (A<sub>T</sub>), and (c) pH (± standard deviations) in the surface water after rewetting, as measured from December 2019 to December 2020. Data from the flooded peatland (n = 6) are shown in blue and data from the inner bay (until 11 March 2020: n = 1, thereafter: n = 2) in black. The vertical black line indicates the rewetting event.

### 3.3.2 CH<sub>4</sub>

During the first few months after flooding (in winter), the CH<sub>4</sub> concentrations in both the inner bay and the peatland were low and did not differ significantly (Figure 7b, Table 2): 48.0 ± 49.5 nmol L<sup>-1</sup> (peatland) and 81.4 ± 107.0 nmol L<sup>-1</sup> (inner bay). From mid-spring onwards, CH<sub>4</sub> concentrations in the inner bay and the peatland increased such that during summer and autumn 2020, the differences at the two areas were significant (*p* < 0.05). Mean CH<sub>4</sub> values were highest in summer and amounted 1502.4 ± 693.4 nmol L<sup>-1</sup> in the peatland and 502.5 ± 479.3 nmol L<sup>-1</sup> in the inner bay. Further, the peatland was characterized by a considerable short-term variability in spring and summer, expressed in four peaks representing elevated concentrations. A positive significant correlation (*r*<sub>S</sub> = 0.73, n = 72, *p* < 0.001) was found in the peatland between the surface water CH<sub>4</sub> concentrations and a water temperature > 10 °C, but not < 10 °C.



470

**Figure 7.** Time series of the mean (a) pCO<sub>2</sub>, (b) CH<sub>4</sub> concentration (cCH<sub>4</sub>), and (c) N<sub>2</sub>O concentration (cN<sub>2</sub>O) (± standard deviations) after rewetting in the surface water from December 2019 to December 2020. Data from the flooded peatland (n = 6) are shown in blue and data from the inner bay (until 11 March 2020: n = 1, thereafter: n = 2) in black. The vertical black line indicates the rewetting event.

### 3.3.3 N<sub>2</sub>O

475 The highest N<sub>2</sub>O concentration of 486.3 nmol L<sup>-1</sup> was measured in the peatland one week after rewetting (Figure 7c), followed by 4–5 weeks of still elevated N<sub>2</sub>O concentrations between 19.9 and 91.8 nmol L<sup>-1</sup>. During winter, significant positive correlations were determined in the peatland between N<sub>2</sub>O and NH<sub>4</sub><sup>+</sup> ( $r_s = 0.61$ ,  $n = 45$ ,  $p < 0.001$ ) and between N<sub>2</sub>O and NO<sub>2</sub><sup>-</sup> ( $r_s = 0.46$ ,  $n = 45$ ,  $p < 0.01$ ). From spring onwards, N<sub>2</sub>O decreased rapidly, both in the peatland and the inner bay, with the lowest values of 4.7 to 7.9 nmol L<sup>-1</sup> reached in summer. Other positive correlations of N<sub>2</sub>O with N-nutrients in the peatland  
480 included NO<sub>3</sub><sup>-</sup> ( $r_s = 0.74$ ,  $n = 35$ ,  $p < 0.001$ ) and NO<sub>2</sub><sup>-</sup> ( $r_s = 0.70$ ,  $n = 35$ ,  $p < 0.001$ ) in spring and all N species in autumn (NO<sub>3</sub><sup>-</sup>:  $r_s = 0.85$ ,  $n = 30$ ,  $p < 0.001$ ; NO<sub>2</sub><sup>-</sup>:  $r_s = 0.70$ ,  $n = 30$ ,  $p < 0.001$ ; NH<sub>4</sub><sup>+</sup>:  $r_s = 0.80$ ,  $n = 30$ ,  $p < 0.001$ ).

Spatial differences in N<sub>2</sub>O concentrations between the inner bay and the peatland were low and not significant in winter, spring or autumn, whereas significantly lower concentrations were measured in the peatland during summer (Table 2).

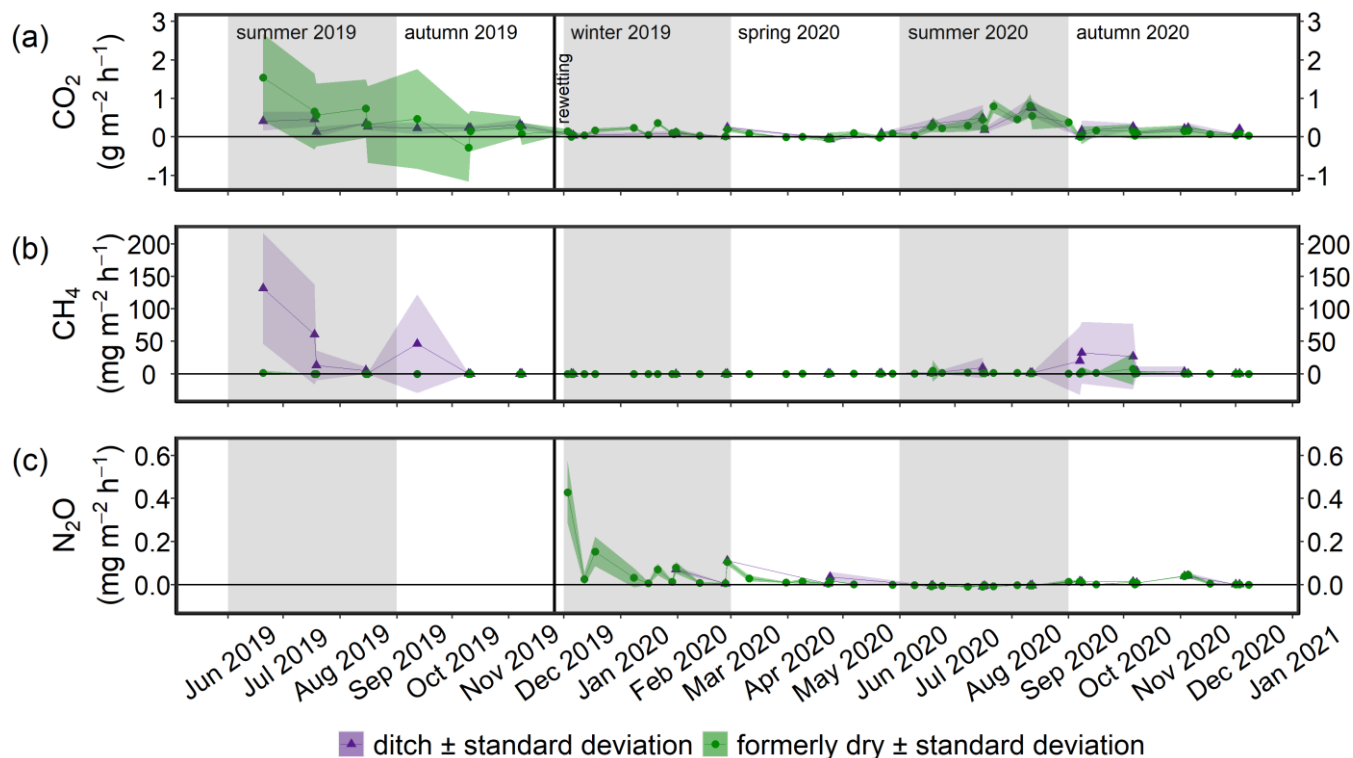
### 3.4 Pre- and post-rewetting GHG fluxes (CO<sub>2</sub>, CH<sub>4</sub>, N<sub>2</sub>O)

485 Terrestrial CO<sub>2</sub> fluxes before rewetting, during summer and autumn 2019, were highly variable ranging from -3.3 to 3.0 g m<sup>-2</sup> h<sup>-1</sup> with a mean ± SD of 0.29 ± 0.82 g m<sup>-2</sup> h<sup>-1</sup> (Figure 8a). Within the ditch, pre-rewetting CO<sub>2</sub> fluxes ranged from -0.008 to 0.6 g m<sup>-2</sup> h<sup>-1</sup>, but on average were comparable to the fluxes determined at the terrestrial (dry) surface.

After rewetting, formerly terrestrial CO<sub>2</sub> fluxes decreased in amplitude (-0.5 to 1.4 g m<sup>-2</sup> h<sup>-1</sup>), while the summer and autumn averages were unchanged compared to the pre-rewetting fluxes (Table 3). In the ditch, the mean and minimum post-  
490 rewetting CO<sub>2</sub> fluxes were within the range of those determined pre-rewetting (mean: 0.26 ± 0.29 g m<sup>-2</sup> h<sup>-1</sup>, min: -0.02 g m<sup>-2</sup> h<sup>-1</sup>) but the maximum flux (1.1 g m<sup>-2</sup> h<sup>-1</sup>) was almost twice as high as the pre-rewetting ditch flux (max: 0.6 g m<sup>-2</sup> h<sup>-1</sup>).

Pre-rewetting CH<sub>4</sub> fluxes (mean ± SD) in summer and autumn 2019 varied between -0.9 to 8.4 mg m<sup>-2</sup> h<sup>-1</sup> (terrestrial) and -1.1 to 193.6 mg m<sup>-2</sup> h<sup>-1</sup> (drainage ditch; Figure 8b). While mean terrestrial CH<sub>4</sub> fluxes were 0.13 ± 1.01 mg m<sup>-2</sup> h<sup>-1</sup>, the  
495 mean ditch fluxes were 11.4 ± 37.5 mg m<sup>-2</sup> h<sup>-1</sup>. In summer and autumn 2020, after rewetting, average CH<sub>4</sub> fluxes on formerly terrestrial land increased slightly but significantly (1.74 ± 7.59 mg m<sup>-2</sup> h<sup>-1</sup>), whereas in the ditch they decreased considerably (8.5 ± 26.9 mg m<sup>-2</sup> h<sup>-1</sup>). Flux amplitudes at the ditch station before and after rewetting were comparable.

Data on N<sub>2</sub>O fluxes are available only for the post-rewetting period. The rewetted peatland was a small source of N<sub>2</sub>O, with an annual mean (± SD) flux of 0.02 ± 0.07 mg m<sup>-2</sup> h<sup>-1</sup> in the first year after rewetting (Figure 8c). The highest N<sub>2</sub>O  
500 flux of 0.4 mg m<sup>-2</sup> h<sup>-1</sup> occurred one week after rewetting, followed by lower N<sub>2</sub>O fluxes between 0.007 and 0.2 mg m<sup>-2</sup> h<sup>-1</sup> within the following 4–5 weeks. Afterwards, N<sub>2</sub>O fluxes remained constantly close to zero. Negative fluxes, indicating N<sub>2</sub>O uptake, were measured only in summer.



505 **Figure 8.** Time series of the mean (a) CO<sub>2</sub>, (b) CH<sub>4</sub>, and (c) N<sub>2</sub>O fluxes ( $\pm$  standard deviations) from June 2019 to December 2020. Fluxes of the permanently wet drainage ditch are shown in purple and those derived from the two methods employed in this study in green. The vertical black line indicates the rewetting event.

## 4. Discussion

### 4.1 Nutrient dynamics and export

510 The seasonal dynamics of the nutrients followed a typical course over the year. Thus, after rewetting, NH<sub>4</sub><sup>+</sup>, NO<sub>3</sub><sup>-</sup>, and NO<sub>2</sub><sup>-</sup> concentrations in the water column were high in winter and autumn, which is typically due to the mineralization of OM followed by nitrification (Voss et al., 2010). By contrast, the low DIN concentrations during spring and summer reflected the consumption of nutrients by plants and phytoplankton. The very high chlorophyll a concentration (up to 125  $\mu$ g L<sup>-1</sup>) in the peatland indicated the presence of a highly phototrophic community, likely driven by the higher availability of nutrients compared to the inner bay. Due to these distinct seasonal differences with the lowest nutrient concentrations in spring and summer, a rewetting within these seasons would probably be more beneficial to reduce a potential nutrient export into the inner bay, at least during the first few months after rewetting.

515 To assess whether the flooded peatland served as a nutrient source for the inner bay, nutrient concentrations of the peatland were compared with those of the inner bay and of an unaffected monitoring station (“central bay”) and showed generally higher mean concentrations. Due to drainage, the mineralization of upper peat layers can lead to an accumulation of

520 nutrients within the soil (Zak and Gelbrecht, 2007; Cabezas et al., 2012). After rewetting, nutrient concentrations in the  
porewater and ultimately in the overlying water increase (van de Riet et al., 2013; Harpenslager et al., 2015; Zak et al., 2017).  
The leaching of nutrients is driven by concentration differences across the soil-water interface, but it is also dependent on  
factors such as salinity (Rysgaard et al., 1999; Steinmuller and Chambers, 2018), the oxygen availability in the soil (Lennartz  
and Liu, 2019), and the effects of the latter on microbial processes (Burgin and Groffman, 2012), as well as on the degree of  
525 peat decomposition (Cabezas et al., 2012). For instance, highly degraded peat, such as at our study area, can store and release  
more nutrients than less degraded peat (Cabezas et al., 2012), meaning that the highly degraded peat of our study area was  
prone to leach high amounts of nutrients. Occasional measurements of porewater nutrient concentrations in the peat of our  
study area revealed DIN and  $\text{PO}_4^{3-}$  concentrations up to one order of magnitude higher than those in the surface water (Anne  
Breznikar, unpublished data), providing further support for the leaching of nutrients out of the peatland and into the inner bay.

530 The estimated annual nutrient exports (mean  $\pm$  95 % confidence level) from the peatland of  $10.8 \pm 17.4 \text{ t yr}^{-1}$  DIN-N  
and  $0.24 \pm 0.29 \text{ t yr}^{-1}$   $\text{PO}_4\text{-P}$  (peatland/inner bay) and  $33.8 \pm 9.6 \text{ t yr}^{-1}$  DIN-N and  $0.09 \pm 0.32 \text{ t yr}^{-1}$   $\text{PO}_4\text{-P}$  (peatland/central  
bay) were high, given the small size of the flooded peatland ( $\sim 0.5 \text{ km}^2$  at 0 masl). For comparison, the Warnow, a small river  
that flows into the Baltic Sea near the city of Rostock, Mecklenburg-Vorpommern, draining an area of  $\sim 3300 \text{ km}^2$ , had a mean  
annual DIN-N and  $\text{PO}_4\text{-P}$  export of  $1200 \pm 500 \text{ t yr}^{-1}$  and  $19.9 \pm 7.6 \text{ t yr}^{-1}$ , respectively, over the last 25 years (HELCOM,  
535 2019). Therefore, the total nutrient export from the flooded peatland to the inner bay and to the central bay in the first year  
after rewetting accounted for  $\sim 1$  and  $\sim 3$  %, respectively, of the annual DIN-N and  $\text{PO}_4\text{-P}$  loads of the Warnow. When  
normalized to the same dimensions, our study area exported  $21.6\text{--}67.6 \text{ t DIN-N km}^{-2} \text{ yr}^{-1}$  and  $0.18\text{--}0.48 \text{ t PO}_4\text{-P km}^{-2} \text{ yr}^{-1}$ ,  
whereas the Warnow exported only  $0.36 \text{ t DIN-N km}^{-2} \text{ yr}^{-1}$  and  $0.01 \text{ t PO}_4\text{-P km}^{-2} \text{ yr}^{-1}$ .

However, we also want to shortly address the reasons for the high uncertainty range of our calculated nutrient exports.  
540 Firstly, they derive from high fluctuating nutrient concentrations in the surface water within the seasons. This is also visible in  
the high standard deviations (Table 2). Therefore, the 95 % confidence level of the nutrient exports is high and reflects the  
natural dynamic. Secondly, we conducted default error propagation during the export calculation which leads to even higher  
ranges on top of the high natural dynamic.

Compared to the Warnow river, it is noticeable that the range of uncertainties is highly different for the two sources.  
545 While our uncertainties are mostly higher and in the same order of magnitude compared to the means, the uncertainties of the  
river data are one order of magnitude lower. This is likely due to the different time scales of the two data sets. Our export data  
were generated by taking only the first post-rewetting year into account in which the system was still in a transition state and  
thus, showed very dynamic nutrient concentrations. The uncertainties of the river exports were generated by using 25 years of  
data, leading to lower uncertainties than using data from only one year and they were calculated as standard deviation and not  
550 as 95 % confidence level, as was done for the exports of our study site. Therefore, this has to be considered when their  
uncertainty ranges are compared directly. Nevertheless, our results highlight the importance of currently still unmonitored and  
small, independent draining areas along the coastline of the Baltic Sea, in particular those that become intentionally flooded  
(HELCOM, 2019).

## 4.2 Assessment of the GHG dynamics

### 555 4.2.1 CO<sub>2</sub>

The carbon system in our study area is governed by a variety of processes (e.g. Wolf-Gladrow et al., 2007; Kuliński et al., 2017; Schneider and Müller, 2018). C<sub>T</sub> and A<sub>T</sub> were transported with the brackish water from the central bay and ultimately from the Arkona Basin. Additional alkalinity can be added either by a supply of freshwater, which in the southwestern Baltic Sea is characterized by higher alkalinities than the brackish or even saltwater endmember (Beldowski et al., 2010; Müller et al., 2016), or can be introduced by mineralization processes from the seafloor in the inner bay and the flooded peatland. Primary production (i.e., carbon fixation) will decrease C<sub>T</sub>, lower the pCO<sub>2</sub> and increase pH during the formation of organic matter. The mineralization of OM from various sources (new primary production, mineralization of the inundated former vegetation and from the underlying peat) will enhance C<sub>T</sub> and A<sub>T</sub> concentrations, increase pCO<sub>2</sub> and decrease pH. Air-sea exchange during our study is fostered by a pCO<sub>2</sub> that is above atmospheric levels throughout the year, except for a short period in spring in the inner bay and the peatland, where outgassing of CO<sub>2</sub> occurred, resulting in lower pCO<sub>2</sub> and a decrease in C<sub>T</sub>.

We observed three main developments in the surface water CO<sub>2</sub> system and air-sea flux pattern: (i) in winter 2019/2020, the CO<sub>2</sub> system hardly differed between the peatland and the inner bay; (ii) from spring to autumn, there were significant differences in the CO<sub>2</sub> system between the peatland and the inner bay, with higher pCO<sub>2</sub>, C<sub>T</sub> and A<sub>T</sub> values and lower pH in the peatland coinciding with an enrichment in chlorophyll a; (iii) overall, the first post-rewetting year showed sustained high, but less variable CO<sub>2</sub> fluxes compared to pre-rewetting conditions. In the following, we will discuss these three observations and set them into context.

#### 4.2.1.1 Initial post-rewetting CO<sub>2</sub> dynamics

The first weeks after the rewetting were characterized by high nutrient concentrations, a continuous increase in A<sub>T</sub>, C<sub>T</sub> and pH and a decrease in pCO<sub>2</sub> (Figure 4, Figure 6, Figure 7). The increase in C<sub>T</sub> and A<sub>T</sub> coincided with a steady increase in salinity (Figure 3), which is in line with a general increase of A<sub>T</sub> with increasing salinity known for the western Baltic Sea (e.g. Kuliński et al., 2022).

Still, the A<sub>T</sub> values at the given salinity were higher in the inner bay and the peatland than would be expected from a linear A<sub>T</sub>/salinity relation found for surface waters in the open Baltic Sea from the central Gotland Sea to the Kattegat (Beldowski et al., 2010; Müller et al., 2016). Thus, the high A<sub>T</sub> in the inner bay and peatland were likely associated with local carbonate (CaCO<sub>3</sub>) weathering from terrestrial sources and/or a transport by groundwater (Schneider and Müller, 2018). C<sub>T</sub> and A<sub>T</sub> values during this period were consistently higher by ~70–80 μmol kg<sup>-1</sup> in the peatland than in the inner bay, consistent with enhanced leaching from the recently inundated peat. Besides, local CaCO<sub>3</sub> weathering as well as local anoxic processes, such as SO<sub>4</sub><sup>2-</sup> reduction may have increased the A<sub>T</sub> in the submerged soil and finally contributed to higher A<sub>T</sub> values compared to the inner bay.

The oversaturation in pCO<sub>2</sub> and potentially the excess leaching of alkalinity from the soil might have contributed to the decrease in pCO<sub>2</sub> and increase in pH in the peatland in winter 2019/2020. This was apparently reinforced by a short episode



of primary production mid/end January, indicated by a steeper decline of the pCO<sub>2</sub> and a steeper pH increase. This coincided with a short increase in chlorophyll a (~30 µg L<sup>-1</sup>) and a slight intermittent increase of the surface water temperatures (Figure 3). This short, unusually early productive period might have resulted from the high nutrient availability induced by the rewetting of the peatland (Sect. 3.2.1), in particular the high NH<sub>4</sub><sup>+</sup> levels, which simultaneously showed a sharp intermittent minimum.

#### 4.2.1.2 The predominance of production and mineralization shaped the productive period (spring to autumn)

In late winter and the first half of spring, pCO<sub>2</sub> continuously decreased in the peatland as well as in the inner bay. Lowest pCO<sub>2</sub> was measured between March and May and coincided with enhanced chlorophyll a concentrations and a high availability of nutrients in the peatland and in the inner bay, which decreased until mid spring. This resulted in a slight CO<sub>2</sub> uptake in the peatland of -0.005 g m<sup>-2</sup> h<sup>-1</sup> for a short period of time, so that spring was the only season when pCO<sub>2</sub> was on average below atmospheric concentrations in the inner bay (Figure 8). This finding can be attributed to the onset of the productive period, at still moderate surface water temperatures below 10 °C until mid April. During this period, productivity clearly exceeded mineralization, as suggested by the decreasing pCO<sub>2</sub> and increasing pH, despite rising temperatures, as well as increasing O<sub>2</sub> oversaturation in the surface waters. These trends were slightly more pronounced in the peatland than in the inner bay, in accordance with higher nutrient concentrations available for production.

From mid spring until late summer, the peatland was characterized by increased pCO<sub>2</sub> and a variable CO<sub>2</sub> system together with high mean chlorophyll a concentrations of up to 106.0 µg L<sup>-1</sup>. N-nutrients were very low and the system was clearly nitrogen-limited, with only slightly elevated NH<sub>4</sub><sup>+</sup> concentrations in late summer (Figure 3, Figure 4). Furthermore, the O<sub>2</sub> saturation shifted from over- to undersaturated conditions. These observations suggest that the peatland and the inner bay were characterized by simultaneous production and mineralization processes from mid spring until autumn that kept the N-nutrients (except PO<sub>4</sub><sup>3-</sup>) low. Mineralization of OM in the water column, sediment and soil dominated over production, leading to the observed high pCO<sub>2</sub>, lowered pH, and enhanced A<sub>T</sub> and C<sub>T</sub> concentrations. Mineralization during this period was more pronounced in the peatland than in the inner bay, leading to the higher pCO<sub>2</sub>, A<sub>T</sub>, and C<sub>T</sub> values in the peatland, and a stronger and more pronounced reduction of the pH. This stronger mineralization, in particular in the warm summer months, also led to higher DOC concentrations in summer, with a maximum in June/July coinciding with maximum surface water temperatures. The enhanced mineralization in the peatland was likely fueled by higher OM availability from high decomposition rates of fresh plant substrate from inundated plant residuals (Glatzel et al., 2008; Hahn-Schöfl et al., 2011). In addition, aerobic and anaerobic oxidation of CH<sub>4</sub>, that was produced in anoxic zones, might have led to increased CO<sub>2</sub> production, especially during increased water temperatures (e.g. Treude et al., 2005; Dean et al., 2018), due to the availability of SO<sub>4</sub><sup>2-</sup> and O<sub>2</sub>.

The calculated A<sub>T</sub> (from C<sub>T</sub> and pH) in the peatland was consistently lower than the measured A<sub>T</sub> with a difference in the range of 55–122 µmol kg<sup>-1</sup> and thus of 2.7–4.7 % (data not shown). This difference was higher than in the Baltic Sea, where the contribution of organic A<sub>T</sub> is estimated to be 1.5–3.5% (Kuliński et al., 2014). Due to closer vicinity to the coast and the high amount of degradable OM, this higher contribution of organic A<sub>T</sub> was to be expected. The highest discrepancy between measured A<sub>T</sub> values and those calculated from pH and C<sub>T</sub> occur in early summer, simultaneously to the highest values in DOC,

in particular in the peatland (Figure 3). This suggests that the organic  $A_T$  related to the occurrence of DOC (and thus dissolved organic matter (DOM)), contributed to the excess of  $A_T$ . The higher DOM formation in summer in the peatland might partly explain the difference in  $A_T$  between the inner bay and the peatland.

#### 4.2.1.3 Brackish water flooding caused sustained high but less variable $CO_2$ fluxes

625 The amplitude of the  $CO_2$  fluxes from formerly drained parts of the study area decreased after rewetting with brackish water, while the amplitude of  $CO_2$  fluxes from the ditch (inundated after flooding but with deeper, probably incompletely exchanged water) did not differ strongly before and after rewetting (Figure 8). An increased water table is the main driver for the reduction of  $CO_2$  emissions on formerly drained locations. A similar scenario has been reported for terrestrial sites (Bubier et al., 2003; Strack, 2008). In a nearby coastal peatland, both photosynthesis and ecosystem respiration were strongly reduced after  
630 rewetting (Koebsch et al., 2013). The rewetting of our study area probably caused a die-back of the highly productive grassland vegetation, which most likely lead to a reduction of the  $CO_2$  flux amplitude.

Average summer/autumn  $CO_2$  fluxes after rewetting had a mean of  $0.26 \pm 0.29 \text{ g m}^{-2} \text{ h}^{-1}$  and remained thus relatively high compared with those fluxes from 2019. They were also higher than the fluxes determined in studies of shallow coastal or near-shore waters in the northwestern Bornholm Sea of up to  $0.01 \text{ g m}^{-2} \text{ h}^{-1}$  (Thomas and Schneider, 1999) or the Bothnian  
635 Bay of around  $\sim 0.0007 \text{ g m}^{-2} \text{ h}^{-1}$  (Löffler et al., 2012). In a nearby coastal fen recently influenced by brackish water inflow, ecosystem respiration was two orders of magnitude lower (Koebsch et al., 2020) compared to our study site, where the ongoing decomposition of submerged substrate from plant residuals and the fresh soil may have fueled the continuously high  $CO_2$  fluxes in the first year after rewetting (Hahn-Schöfl et al., 2011). The mineralization of OM from primary production driven by the high initial nutrient availability, as well as aerobic and anaerobic oxidation (Dean et al., 2018) of easily degradable  
640 substrates or  $CH_4$ , might have additionally contributed to these  $CO_2$  fluxes. We expect that  $CO_2$  emissions will further decrease, likely because substrates become exhausted and a novel ecosystem will be established (Kreyling et al., 2021), with developing algae fostering  $CO_2$  fixation.

#### 4.2.2 $CH_4$

We observed three main developments in surface water methane concentrations and flux patterns: (i) a short-term, very  
645 moderate increase in  $CH_4$  concentrations directly after rewetting in winter 2019/2020; (ii) an increase in the  $CH_4$  concentrations mainly from spring to autumn, that was significantly higher and more variable in the peatland than in the inner bay and correlated with water temperature; (iii) in the first year after rewetting, much lower  $CH_4$  fluxes than reported for nearby peatlands rewetted by freshwater. These three observations are discussed and set into context in the following.

##### 4.2.2.1 Short-term, moderate increase in the $CH_4$ concentrations in the winter after rewetting

650 The measurements in winter, immediately after rewetting, showed a short-term but moderate increase in the  $CH_4$  concentrations (Figure 7). The rewetting resulted in inundation of the degraded peat and the remaining vegetation. Therefore, it is assumed that methanogenesis was not limited by the availability of high-quality OM, which is often a major controlling factor (Heyer and Berger, 2000; Parish, 2008), and likely originated from decomposition of the residual plant material.

655 However, since CH<sub>4</sub> concentration remained low, a temperature control is assumed, which has been frequently described in the literature. A major control of temperature has been reported, for example, for a nearby shallow coastal area of the Baltic Sea, between the islands of Rügen and Hiddensee, where low CH<sub>4</sub> emission rates and variability were found together with low temperatures (Heyer and Berger, 2000).

660 The rewetting with brackish water transported water with a salinity of 6–7.4 into the peatland such that there were no significant differences in salinity compared to the inner bay in winter (same as for temperature; Table 2). Thus, sulfate reached the peatland immediately after rewetting. As a terminal electron acceptor (TEA), SO<sub>4</sub><sup>2-</sup> promotes the activity of sulfate-reducing bacteria (SRB), which outcompete methane-producing microorganisms (methanogens) for substrates (Segers and Kengen, 1998; Jørgensen, 2006; Segarra et al., 2013). This process was shown to play an important role in flat brackish water systems (e.g. Heyer and Berger, 2000). The availability of other TEAs, such as NO<sub>3</sub><sup>-</sup> that had high concentrations of ~100 ± 58 μM in our study, could have further suppressed methanogenesis (Table 2) (Jørgensen, 2006). Beside competitive 665 mineralization, aerobic and anaerobic CH<sub>4</sub> oxidation may have reduced the CH<sub>4</sub> concentrations (Heyer and Berger, 2000; Reeburgh, 2007; Knittel and Boetius, 2009; Steinle et al., 2017), supported by the effective exchange of water masses. Overall, the rewetting with brackish water during the cold winter season apparently inhibited methanogenesis and/or facilitated effective CH<sub>4</sub> oxidation, resulting in low CH<sub>4</sub> concentrations and a small CH<sub>4</sub> flux into the atmosphere.

#### 4.2.2.2 Increased and variable CH<sub>4</sub> concentrations during the vegetation period

670 The temperature increase from spring to autumn was accompanied by elevated, albeit variable, CH<sub>4</sub> concentrations. Temperature is of crucial importance in controlling the CH<sub>4</sub> cycle in shallow coastal brackish water (Bange et al., 1998; Heyer and Berger, 2000) and in the North Sea (e.g. Borges et al., 2018). Similar relationships have been described for wetlands, e.g. for permanently inundated wetlands (e.g. Koebsch et al., 2015) and in a peatland close to our study site during the first year after rewetting (Hahn et al., 2015). Accordingly, CH<sub>4</sub> concentrations in the peatland ( $r_s = 0.75$ ,  $n = 74$ ,  $p < 0.05$ ) and the inner 675 bay ( $r_s = 0.55$ ,  $n = 29$ ,  $p < 0.05$ ) also correlated significantly and positively with temperature. In the study of Heyer and Berger (2000) the temperature range influenced the temporal variability in CH<sub>4</sub> emissions, which were highest in late spring. Since the temperature range in the peatland of our study was variable (e.g. maximum difference of ~6 °C between samplings), with the highest values between spring and autumn (7.4–23.1 °C), this variability may have strongly contributed to the observed CH<sub>4</sub> dynamics.

680 The peatland and the inner bay were clearly influenced by the same hydrographic conditions, evidenced by their very similar salinities and temperatures. However, the peatland showed higher CH<sub>4</sub> concentrations from spring to late autumn, likely due to the high availability of OM as described by Heyer and Berger (2000) and Bange et al. (1998). Incubation experiments of a degraded fen grassland demonstrated the accumulation of fresh plant litter in a new sediment layer after flooding that resulted in high rates of CH<sub>4</sub> and CO<sub>2</sub> production (Hahn-Schöfl et al., 2011). A further potential driver of OM 685 availability is the sedimentation of freshly produced OM originating from primary production, as described for shallow areas in the Baltic Sea (Bange et al., 1998) and for a shallow bight in the North Sea, which in the latter led to a yearly peak in the seasonal CH<sub>4</sub> cycle (Borges et al., 2018). Although our observations were not made in OM-poor sediments, an impact of

freshly produced OM on enhanced CH<sub>4</sub> concentrations in the OM-rich Drammendorf peatland is possible, given the significant positive correlation of the surface CH<sub>4</sub> concentrations and the chlorophyll a concentration ( $r_s = 0.41$ ,  $n = 56$ ,  $p < 0.05$ ).

#### 690 4.2.2.3 Brackish water rewetting and low CH<sub>4</sub> emissions

Despite high surface water CH<sub>4</sub> concentrations in the peatland and their inter-seasonal and spatial variability, rewetting with brackish water resulted in CH<sub>4</sub> emissions considerably lower than those from temperate fens rewetted with freshwater, where CH<sub>4</sub> emissions strongly increased (Augustin and Chojnicki, 2008; Couwenberg et al., 2011; Hahn et al., 2015; Franz et al., 2016; Jurasinski et al., 2016).

695 At our study site, although average CH<sub>4</sub> fluxes on formerly terrestrial locations increased significantly by one order of magnitude after rewetting, the overall increase from  $0.13 \pm 1.01$  to  $1.74 \pm 7.59$  mg m<sup>-2</sup> h<sup>-1</sup> (Figure 8) was lower than that reported for freshwater rewetted fens under similar climatological boundary conditions (e.g. Hahn et al., 2015; Franz et al., 2016). Even several years after rewetting, the annual CH<sub>4</sub> budgets of a shallow lake on a formerly drained fen varied between 13.2 and 52.6 g m<sup>-2</sup> yr<sup>-1</sup> (Franz et al., 2016), which corresponds to approximately 1.5 to 6.0 mg m<sup>-2</sup> h<sup>-1</sup>. Our CH<sub>4</sub> fluxes were  
700 also lower than the emissions reported from coastal-near shallow waters of the Baltic Sea, where fluxes of 39.9–104.2 mg m<sup>-2</sup> h<sup>-1</sup> were measured in June/July (Heyer and Berger, 2000). For the same months, mean CH<sub>4</sub> fluxes at the formerly dry stations in our study site were 0.5–4.9 mg m<sup>-2</sup> h<sup>-1</sup>. However, compared to CH<sub>4</sub> fluxes from continental shelves (0.015–0.024 mg m<sup>-2</sup> h<sup>-1</sup>; adapted from Bange et al., (1994)), the fluxes of our study site were two orders of magnitude higher. Despite low average fluxes, emission peaks could be distinguished with the highest flux from the now inundated ditch of  
705 149.2 mg m<sup>-2</sup> h<sup>-1</sup> in September 2020 and 108.3 mg m<sup>-2</sup> h<sup>-1</sup> in October 2020. While these values were still lower than the maximum value of 243.0 mg m<sup>-2</sup> h<sup>-1</sup> reported by Heyer and Berger (2000), it is important to stress that our study site was a source of CH<sub>4</sub> already in its drained state, especially within the drainage ditch, where CH<sub>4</sub> fluxes were comparable to the ~0.2 mg m<sup>-2</sup> h<sup>-1</sup> reported from undrained fens (Danevčič et al., 2010).

The lower CH<sub>4</sub> emissions of the brackish rewetted Drammendorf peatland might be attributed to the availability of  
710 TEAs, especially SO<sub>4</sub><sup>2-</sup>, which (1) may have contributed to a suppression in methanogenesis by competitive inhibition (Segers and Kengen, 1998; Jørgensen, 2006; Segarra et al., 2013) or (2) fostered the anaerobic oxidation of methane (AOM) as an effective pathway to reduce CH<sub>4</sub> emissions, and by (3) fast aerobic CH<sub>4</sub> oxidation mediated by oxygen-rich water. The high variability of CH<sub>4</sub> concentrations may also be related to changing rates of AOM, as the process is sensitive to the introduction of O<sub>2</sub> mediated by sporadic wind-driven resuspension (Treude et al., 2005). Since our study area was shallow and likely  
715 experiences regular wind-driven resuspension, spatially and temporally dynamic AOM can be assumed. The low CH<sub>4</sub> fluxes suggested that effective aerobic and anaerobic oxidation of CH<sub>4</sub> likely occurred. Moreover, higher CH<sub>4</sub> concentrations in the peatland compared to the inner bay in combination with the high lateral water exchange due to frequent changes in the water level (Figure A3) should have driven a net advective export of CH<sub>4</sub>-enriched water to the inner bay. This would have further contributed to the low peatland CH<sub>4</sub> emissions and the observed high variability.

720 While CH<sub>4</sub> production and emission were likely prevented by rewetting with oxygen-rich, sulfate-containing brackish water, the possibility remains that the total CH<sub>4</sub> release was underestimated by insufficient accounting for ebullition. In the

marine environment, bubble-mediated transport is attributed to gassy sediments and an effective mechanism of vertical CH<sub>4</sub> migration (e.g. Borges et al., 2016). Although neither of the methods used to determine CH<sub>4</sub> fluxes specifically account for ebullition, we estimated that 6.9 % of all analyzed chamber-based fluxes were partly bubble-influenced. We estimated this percentage by counting the measurements which showed irregular data points in graphical depiction, but did not influence the linear slope. We observed further that in another 9.6 % of the chamber-based flux measurements the CH<sub>4</sub> concentration patterns indicated ebullition (flux measurements with exponential slope, which was clearly steeper than the linear regression of the majority of data points), but these were not accounted for in the final calculations of diffusive flux. Thus, given that only 16.5 % of the chamber-based flux measurements indicated bubble-mediated CH<sub>4</sub> transport and in almost half of those cases, the resulting perturbation was small and was included in the flux amplitude, the magnitude of the ebullition-driven underestimation of our flux estimates is considered to be small.

In summary, the increase in CH<sub>4</sub> concentrations after rewetting in winter was small, short-lived and associated with the die-back of plants. CH<sub>4</sub> fluxes in the first year after rewetting remained relatively low and were lower than typical for post-rewetting conditions. They also followed a seasonal pattern common for shallow organic-rich systems, with a strong correlation with temperature in spring and summer. We anticipate that continuing reduction in OM availability after the initial die-back of vegetation will likely lead to a further decrease of CH<sub>4</sub> emissions in subsequent years.

### 4.2.3 N<sub>2</sub>O

The rewetted peatland was a source of N<sub>2</sub>O in the first year after rewetting, although the mean annual N<sub>2</sub>O flux of  $0.02 \pm 0.07 \text{ mg m}^{-2} \text{ h}^{-1}$  was very low (Figure 8). This was expected since permanent inundation leads to anoxic conditions in the peat, preventing the production of N<sub>2</sub>O by nitrification, as well as by denitrification due to the lack of NO<sub>3</sub><sup>-</sup> (e.g. Succow and Joosten, 2001; Strack, 2008). However, the range of post-rewetting N<sub>2</sub>O fluxes in the first three months (winter) was clearly much larger than during the rest of the year, which indicated that N<sub>2</sub>O was strongly and immediately affected by the rewetting, as shown elsewhere (Goldberg et al., 2010; Jørgensen and Elberling, 2012). The highest N<sub>2</sub>O flux ( $0.4 \text{ mg m}^{-2} \text{ h}^{-1}$ ) and the highest NH<sub>4</sub><sup>+</sup> concentration (78.0 μM) was measured one week after rewetting and a significant positive correlation between these two variables was found in winter ( $r_s = 0.61$ ,  $n = 45$ ,  $p < 0.001$ ). Additionally, N<sub>2</sub>O correlated significantly positive with NO<sub>2</sub><sup>-</sup> in winter ( $r_s = 0.46$ ,  $n = 45$ ,  $p < 0.01$ ), whereas no correlation with NO<sub>3</sub><sup>-</sup> was found. The accumulation of N<sub>2</sub>O, but also of NO<sub>2</sub><sup>-</sup> and NO<sub>3</sub><sup>-</sup> can generally be interpreted as a result of shifting O<sub>2</sub> conditions in the freshly inundated ecosystem, such that incomplete process chains of e.g. nitrification and denitrification were favored (Rassamee et al., 2011). However, it seems likely that the high N<sub>2</sub>O concentrations in winter originated from nitrification due to the correlations of N<sub>2</sub>O with its substrate (NH<sub>4</sub><sup>+</sup>) and its main accumulating intermediate product (NO<sub>2</sub><sup>-</sup>), as well as a trend of increasing NO<sub>3</sub><sup>-</sup> concentrations throughout the winter.

During late spring and early summer, undersaturation of the surface water with N<sub>2</sub>O, compared to the atmosphere, pointed to consumption within suboxic/anoxic zones of the peat. Consumption in the surface water was unlikely because anoxic conditions were never found near the peat surface. The undersaturation of N<sub>2</sub>O a few months after rewetting evidenced

755 the change in O<sub>2</sub> conditions in the peat, from oxic to hypoxic/anoxic, turning the rewetted peatland into an N<sub>2</sub>O sink, at least temporarily. This change was likely driven by the higher availability of fresh OM (measured as chlorophyll a) in the peatland compared to the inner bay, finally leading to significantly lower N<sub>2</sub>O concentrations in the peatland in summer ( $p < 0.001$ , Table 2).

Previously reported N<sub>2</sub>O fluxes in drained peatlands range from 0.002 to 0.45 mg m<sup>-2</sup> h<sup>-1</sup>, with a clear trend towards  
760 higher fluxes in fertilized or naturally N-rich areas (Flessa et al., 1998; Glatzel and Stahr, 2001; Augustin, 2003; Strack, 2008; Minkkinen et al., 2020). Augustin et al. (1998) examined multiple degraded fens in Mecklenburg-Vorpommern and Brandenburg (Germany) and calculated N<sub>2</sub>O fluxes of 0.04 to 0.10 mg m<sup>-2</sup> h<sup>-1</sup> in extensively and intensively used fen grasslands, respectively (Augustin et al., 1998). N<sub>2</sub>O fluxes in drained peatlands result from a low water level which allows the permanent penetration of atmospheric oxygen into the peat to fuel N<sub>2</sub>O producing processes that are dependent on oxygen  
765 (Martikainen et al., 1993; Regina et al., 1999). As the water level in our study site was permanently below the soil surface before rewetting, it is likely that the drained peat was a source of N<sub>2</sub>O. The mean post-rewetting N<sub>2</sub>O flux determined in our study area ( $0.02 \pm 0.07$  mg m<sup>-2</sup> h<sup>-1</sup>) is in the lower range of reported fluxes from drained peatlands. Therefore, as shown in other studies (Succow and Joosten, 2001; Minkkinen et al., 2020), the rewetting probably led to a reduction of N<sub>2</sub>O fluxes, since they were likely high before the rewetting.

770 In general, the N<sub>2</sub>O fluxes in rewetted peatlands are in the same range as fluxes from pristine ones (Minkkinen et al., 2020), indicating that rewetting is a very effective measure to reduce N<sub>2</sub>O emissions to natural levels. Literature values range from up to 0.01 and 0.02 mg m<sup>-2</sup> h<sup>-1</sup> for rewetted and undrained boreal peatlands (Minkkinen et al., 2020), respectively, to 0.08 mg m<sup>-2</sup> h<sup>-1</sup> for a rewetted riparian wetland near a freshwater meadow (Kandel et al., 2019). Although it is difficult to compare the N<sub>2</sub>O fluxes determined in this study with those from other sites with different salinity, hydrology and history of  
775 use, our mean annual post-rewetting value is in the lower range of N<sub>2</sub>O fluxes previously reported for rewetted and pristine peatlands.

## 5. Conclusions and Outlook

The effects of rewetting a drained coastal peatland with brackish water in winter and the subsequent formation of a permanently inundated area were studied over one year.

780 We found a strong pulse of DIN leaching out of the peat followed by the transport of DIN into the inner bay, leading to a high export especially in winter compared to the Warnow, a nearby river. However, due to a rapid decrease of nutrient concentrations in spring, the nutrient export after a rewetting in spring or summer would likely be lower compared to rewetting in winter, at least during the first few months thereafter.

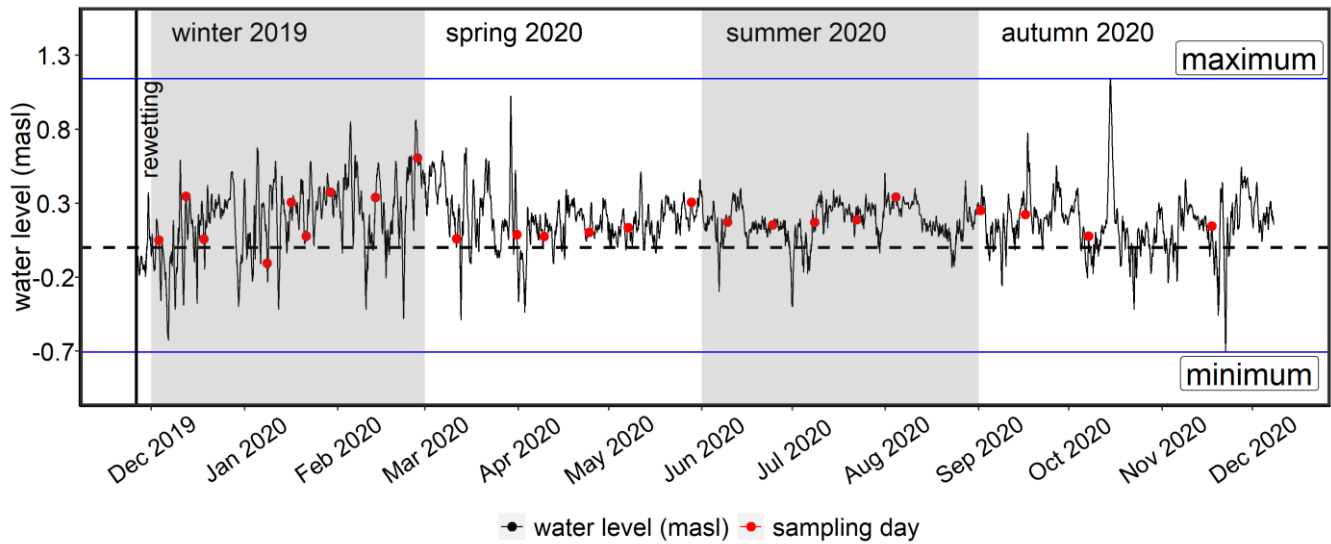
Further, CO<sub>2</sub> concentrations and emissions seem to remain relatively high after the rewetting with brackish water  
785 compared to the dry conditions before rewetting. This was likely driven by the high OM availability from the residual vegetation but also by the high rate of primary production in the water column. However, the flux amplitude decreased after

rewetting and thus, peak emissions during the vegetation period were prevented. The lack of a strong increase of CH<sub>4</sub> emissions in the first year after rewetting with brackish water, in contrast to nearby areas rewetted with freshwater, suggests that especially during the colder months, rewetting with brackish water or seawater would minimize CH<sub>4</sub> emissions and thus maximize the effect on integrated GHG emission reduction. Moreover, a rapid elevation of the water level, as occurred at our study site, will promote the oxidation of peat-derived CH<sub>4</sub> in the water column. Future CH<sub>4</sub> emissions will depend on processes, such as the development of vegetation and will likely decrease. According to literature, dry peatlands were found to be rather large sources of N<sub>2</sub>O due to their drainage for agricultural use. However, the permanent inundation of our study site led to a rapid decrease of N<sub>2</sub>O emissions and converted the peatland into a N<sub>2</sub>O sink during summer, with fluxes similar to pristine peatlands.

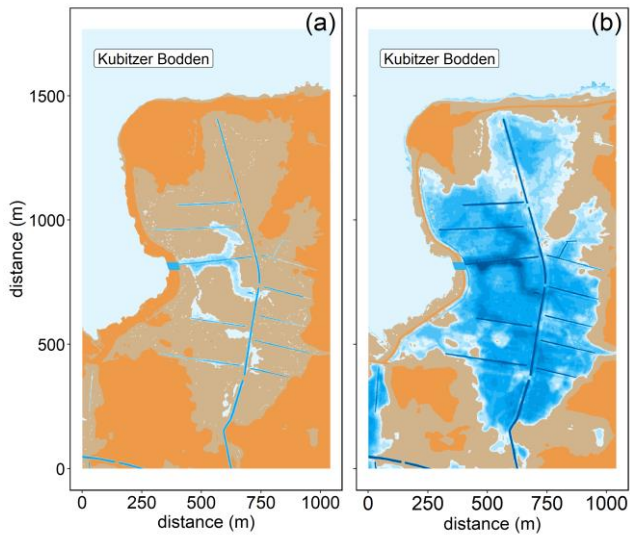
With the ongoing formation of salt grass meadows, livestock farming at our study area can and will continue. However, the area's use has not hindered its positive development towards an ecosystem with the potential to eventually become a carbon and nutrient sink in the future. We expect that both the nutrient export and GHG emissions will slowly decrease due to a shrinking reservoir of substrates. Nonetheless, because degraded peat is both nutrient- and OM-enriched, this decrease will occur slowly, given that the topsoil was not removed prior to flooding to diminish nutrients and OM, as was demonstrated by other studies. Whether or not the area will act as a C sink in the future depends on the success and speed of the establishment of vascular vegetation and its burial in the anoxic parts of the sediment.

Nutrient export from peatlands and the re-establishment of the nutrient and C-sequestration functions of highly degraded coastal peatlands after rewetting are complex processes whose elucidation requires long-term investigations. The pronounced seasonal dynamics highlight the need for approaches that include a high temporal resolution, such as achieved with sensor-based or eddy-supported measurements.

## Appendix A: Study area



810 **Figure A1.** Water level data from the monitoring station “Barhöft” (Wasserstraßen- und Schifffahrtsamt Ostsee), representing the Kubitzer Bodden, from the beginning of rewetting (26 November 2019) until the end of the investigation period. The red dots indicate the sampling days. The dashed horizontal line represents 0 masl. The minimum and maximum water levels of the investigation period are shown by the blue horizontal lines (−0.7 masl and 1.1 masl, respectively). See also Figure A2 and **Figure A3**.



815 **Figure A2.** The changing water level and its effect on the water coverage of the study area, shown for (a) −0.5 masl and (b) 0.5 masl. Topography data retrieved from the Landesamt für innere Verwaltung Mecklenburg-Vorpommern, Amt für Geoinformation, Vermessungs- und Katasterwesen, Fachbereich Geodatenbereitstellung.



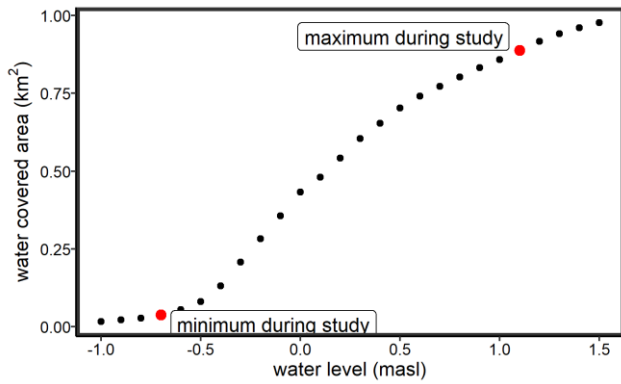


**Figure A3:** Hypsographic curve of the study area, in increments of 0.1 m. The red dots represent the observed range of the water level during the study. For a water level time series during the sampling period, see Figure A1.

## 820 Appendix B: Nutrient export calculation

**Table B1.** Seasonal water volume exchanges ( $Q_{in}/Q_{out}$ ,  $m^3 s^{-1}$ ) and nutrient masses ( $kg m^{-3}$ )  $\pm$  standard error in the inner bay ( $c_{IB}$ ), the central bay ( $c_{CB}$ ), the peatland ( $c_{peatland}$ ), and the resulting net nutrient transport (NNT, in tonnes) for DIN-N and  $PO_4$ -P. Negative values of NNT indicate an export from the peatland into the inner bay/central bay and *vice versa*.

season	$Q_{in}$ ( $m^3 s^{-1}$ )	$Q_{out}$ ( $m^3 s^{-1}$ )	$c_{IB}$	$c_{peatland}$	NNT DIN-N (t)	$c_{IB}$	$c_{peatland}$	NNT $PO_4$ -P (t)
			DIN-N ( $kg m^{-3}$ )	DIN-N ( $kg m^{-3}$ )		$PO_4$ -P ( $kg m^{-3}$ )	$PO_4$ -P ( $kg m^{-3}$ )	
winter	1.9 $\pm 0.1$	-1.9 $\pm 0.1$	$1270 \times 10^{-6}$ $\pm 506 \times 10^{-6}$	$1840 \times 10^{-6}$ $\pm 267 \times 10^{-6}$	$-8.6 \pm 9.9$	$6.5 \times 10^{-6}$ $\pm 5.0 \times 10^{-6}$	$11.5 \times 10^{-6}$ $\pm 3.7 \times 10^{-6}$	$-0.08 \pm 0.10$
spring	1.3 $\pm 0.1$	-1.3 $\pm 0.1$	$243 \times 10^{-6}$ $\pm 289 \times 10^{-6}$	$391 \times 10^{-6}$ $\pm 220 \times 10^{-6}$	$-1.5 \pm 3.8$	$2.8 \times 10^{-6}$ $\pm 2.8 \times 10^{-6}$	$8.1 \times 10^{-6}$ $\pm 3.1 \times 10^{-6}$	$-0.05 \pm 0.04$
summer	1.1 $\pm 0.1$	-1.1 $\pm 0.1$	$44.0 \times 10^{-6}$ $\pm 38.2 \times 10^{-6}$	$82.7 \times 10^{-6}$ $\pm 34.6 \times 10^{-6}$	$-0.3 \pm 0.5$	$6.8 \times 10^{-6}$ $\pm 4.7 \times 10^{-6}$	$15.2 \times 10^{-6}$ $\pm 3.1 \times 10^{-6}$	$-0.07 \pm 0.05$
autumn	1.2 $\pm 0.1$	-1.2 $\pm 0.1$	$301 \times 10^{-6}$ $\pm 218 \times 10^{-6}$	$328 \times 10^{-6}$ $\pm 104 \times 10^{-6}$	$-0.4 \pm 3.2$	$8.1 \times 10^{-6}$ $\pm 6.2 \times 10^{-6}$	$10.9 \times 10^{-6}$ $\pm 3.7 \times 10^{-6}$	$-0.04 \pm 0.10$
<b>total (peatland / inner bay)</b>					$-10.8 \pm 17.4$	$-0.24 \pm 0.29$		
season	$Q_{in}$ ( $m^3 s^{-1}$ )	$Q_{out}$ ( $m^3 s^{-1}$ )	$c_{CB}$	$c_{peatland}$	NNT DIN-N (t)	$c_{CB}$	$c_{peatland}$	NNT $PO_4$ -P (t)
			DIN-N ( $kg m^{-3}$ )	DIN-N ( $kg m^{-3}$ )		$PO_4$ -P ( $kg m^{-3}$ )	$PO_4$ -P ( $kg m^{-3}$ )	
winter	1.9 $\pm 0.1$	-1.9 $\pm 0.1$	$169 \times 10^{-6}$ $\pm 63.1 \times 10^{-6}$	$1840 \times 10^{-6}$ $\pm 267 \times 10^{-6}$	$-26.2 \pm 5.4$	$9.9 \times 10^{-6}$ $\pm 5.9 \times 10^{-6}$	$11.5 \times 10^{-6}$ $\pm 3.7 \times 10^{-6}$	$-0.02 \pm 0.11$
spring	1.3 $\pm 0.1$	-1.3 $\pm 0.1$	$85.1 \times 10^{-6}$ $\pm 42.1 \times 10^{-6}$	$391 \times 10^{-6}$ $\pm 220 \times 10^{-6}$	$-3.1 \pm 2.4$	$4.3 \times 10^{-6}$ $\pm 4.7 \times 10^{-6}$	$8.1 \times 10^{-6}$ $\pm 3.1 \times 10^{-6}$	$-0.04 \pm 0.06$
summer	1.1 $\pm 0.1$	-1.1 $\pm 0.1$	$20.2 \times 10^{-6}$ $\pm 9.5 \times 10^{-6}$	$82.7 \times 10^{-6}$ $\pm 34.6 \times 10^{-6}$	$-0.5 \pm 0.3$	$8.4 \times 10^{-6}$ $\pm 3.4 \times 10^{-6}$	$15.2 \times 10^{-6}$ $\pm 3.1 \times 10^{-6}$	$-0.06 \pm 0.04$
autumn	1.2 $\pm 0.1$	-1.2 $\pm 0.1$	$26.5 \times 10^{-6}$ $\pm 9.1 \times 10^{-6}$	$328 \times 10^{-6}$ $\pm 104 \times 10^{-6}$	$-3.9 \pm 1.5$	$13.0 \times 10^{-6}$ $\pm 6.5 \times 10^{-6}$	$10.9 \times 10^{-6}$ $\pm 3.7 \times 10^{-6}$	$0.03 \pm 0.10$
<b>total (peatland / central bay)</b>					$-33.8 \pm 9.6$	$-0.09 \pm 0.32$		

## Appendix C: Comparability of two independent approaches to atmospheric flux determination

825 Since the gas transfer velocity  $k$  model (Sect. 2.5.3) requires a water-air interface and thus cannot be applied to dry conditions, atmospheric flux measurements obtained by manual closed-chambers along a representative transect (Figure 2b) were available to determine pre-rewetting GHG fluxes ( $\text{CO}_2$  and  $\text{CH}_4$ ). After rewetting, data from manual closed-chambers (transect) and from surface water sampling for the  $k$  model (transect and peatland stations) were used. The two methodologies were applied at the same locations along the transect only after rewetting (Table C1).

830 **Table C1.** Overview of the methods used to determine the atmospheric GHG fluxes

Pre-rewetting	Post-rewetting	
transect (Figure 2b)	transect (Figure 2b)	peatland area (Figure 2a)
chamber-based	chamber-based <sup>1,2</sup>	$k$ model <sup>2</sup>
	$k$ model <sup>1,2</sup>	

<sup>1</sup> inter-methodological comparison at station BTD7  
<sup>2</sup> formed the data representing post-rewetting fluxes

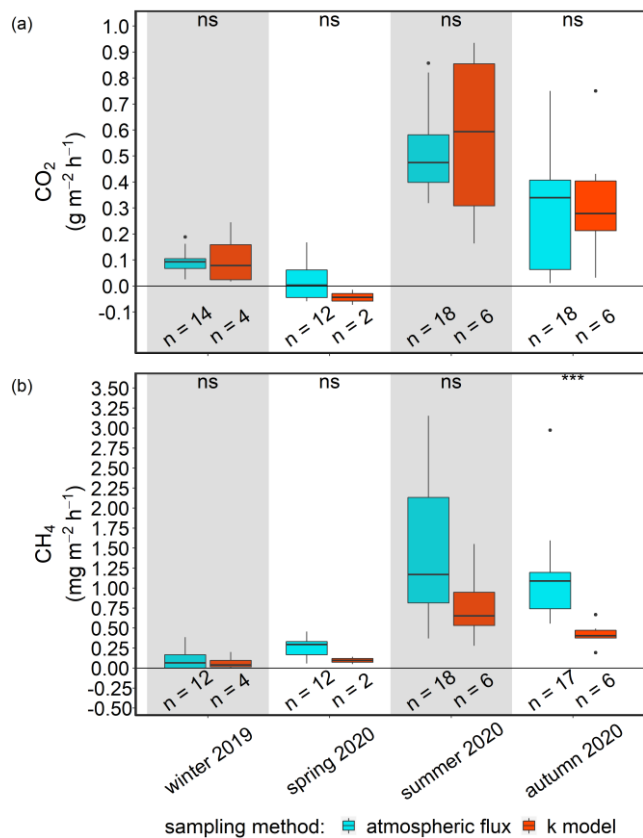
To evaluate the inter-comparability of the flux estimates obtained with the two methods, the results from station BTD7 were compared for each post-rewetting season (Figure C1). Data from this station were chosen because it was permanently flooded after rewetting and thus assured a valid baseline for comparison. The dynamics of the  $\text{CO}_2$  fluxes determined by the two methods were the same and thus did not differ significantly in any of the seasons (Kruskal-Wallis test,  $p > 0.05$ ).

$\text{CH}_4$  fluxes also did not differ significantly, except in autumn (Kruskal-Wallis test,  $p < 0.001$ ), when the average flux calculated according to the two methods differed by a factor of 2.7. However, the data of the  $k$  model had less impact, due to the smaller number of measurements ( $n = 6$ ). Given the smaller data set compared to that of the closed chambers ( $n = 17$ ), the same statistical analysis was conducted without a seasonal division. The results showed no significant differences in the two methods for  $\text{CH}_4$  fluxes (Kruskal-Wallis test,  $\text{CO}_2$  and  $\text{CH}_4$ ). Therefore, it was deemed appropriate to combine the flux-estimation methods for each GHG into one post-rewetting data set, as this allowed the consideration of a broader range of possible flux amplitudes. In addition, the post-rewetting data acquired along the transect were pooled with data distributed throughout the peatland area. Although the area covered by the transect was smaller than the covered by the  $k$ -model data from the peatland, such that pooling of the post-rewetting-data risked spatial bias, two positive effects of pooling were identified:

845 (1) The transect stations were representative of the entire area after flooding, because they covered a water-level-gradient (several cm to  $> 2$  m in the ditch) that coincided with the conditions of the peatland stations. (2) The transect stations represented a large heterogeneity in the peatland before rewetting that decreased post-rewetting. This was also evident from the  $\text{CO}_2$  flux measurements, which showed a high variability (data not shown) at each station before rewetting. After rewetting, there was less variability such that the stations became more similar in their atmospheric C-exchange patterns, likely due to

850 the mixing patterns triggered by lateral exchange with the Baltic Sea (Sect. 3.1). Largely similar conditions were therefore assumed at all stations within the peatland.

The pooled post-rewetting flux values were compared with the pre-rewetting values to investigate the direct effect of rewetting on CH<sub>4</sub> and CO<sub>2</sub> fluxes.



855 **Figure C1.** Seasonal post-rewetting fluxes of (a) CO<sub>2</sub> and (b) CH<sub>4</sub> at station BTD7 which is part of the GHG flux transect. Chamber-based atmospheric GHG fluxes are shown in blue and air-sea GHG fluxes from the k model in red. The methodological comparisons within seasons are based on a significance level of  $p < 0.05$ . ns: not significant; \*\*\*  $p < 0.001$ ).

#### Appendix D: Nutrient cross plots

860 Cross plots with linear regression analyses were generated for nutrients (NH<sub>4</sub><sup>+</sup>, NO<sub>3</sub><sup>-</sup>, NO<sub>2</sub><sup>-</sup>, PO<sub>4</sub><sup>3-</sup>) and DOC concentrations across all seasons to investigate potential correlations (Figure D1). Significant correlations are shown with red asterisks ( $p < 0.05$ ).

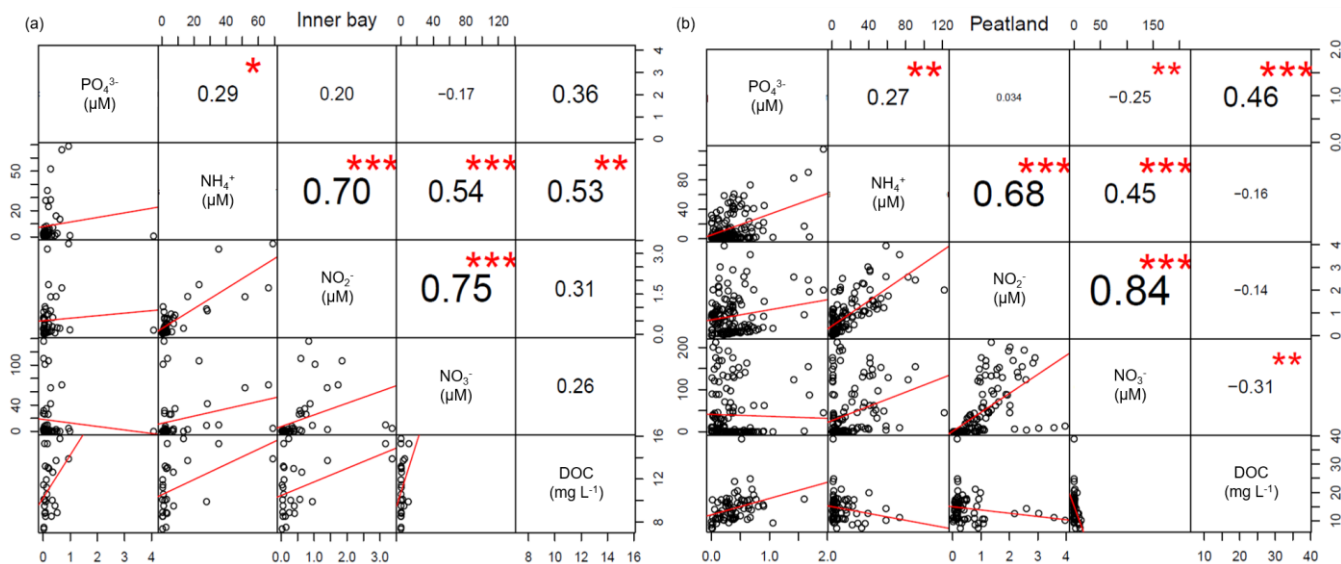


**Figure D1.** Cross plots of the measured nutrient ( $\text{NH}_4^+$ ,  $\text{NO}_3^-$ ,  $\text{NO}_2^-$ ,  $\text{PO}_4^{3-}$ ) and DOC concentrations in (a) the inner bay and (b) the peatland across all seasons. Significant correlations are indicated by asterisks.

865

*Data availability.* The raw data used in this study are archived at <http://doi.io-warnemuende.de/10.12754/data-2022-0003>. The calculated GHG emission data used in this study are archived at <http://doi.io-warnemuende.de/10.12754/data-2022-0004>.

*Author contributions.* All authors designed the concept of the study. DLP, AB and CNG conducted the field work, data analysis, and interpretation. DLP and AB wrote the first draft of the manuscript. DLP created the figures and organized the data. AB conducted the statistical analysis. CNG wrote sections of the manuscript. All authors contributed to manuscript revision and approved the submitted version.

875

*Competing interests.* The authors declare that they have no conflict of interest.

880

*Acknowledgements.* The authors would like to thank Cindy Hoppe and Henning Sack for their great support during the field work; Lara Prella, Petra Mutinova and the Biologische Station Zingst (all University of Rostock) for providing and measuring some additional nutrient data; Christian Burmeister, Dr. Stefan Otto (both IOW) and Dr. Stefan Köhler (University of Rostock) for their technical laboratory assistance; Dr. Joachim Dippner, Dr. Marvin Lorenz and Dr. Christiane Hassenrück (all IOW) for their help on the nutrient export calculation and statistical analyses, respectively. Dr. Bitu Sabbaghzadeh and Dr. Oliver Schmale (both IOW) provided valuable feedback on the manuscript. We are grateful to the Ostseestiftung and especially to Rasmus Klöpffer, who guided the cooperation required for the project and provided valuable data on the study area. We thank Sascha Klatt for information on the study area and especially for technical support during field work. We also thank the

Wasserstraßen- und Schifffahrtsamt Ostsee (WSA Ostsee) for water level data, the Landesamt für innere Verwaltung  
885 Mecklenburg-Vorpommern (LAI V MV), Fachbereich Geodatenbereitstellung for topography data, the Landesamt für Umwelt,  
Naturschutz und Geologie Mecklenburg-Vorpommern (LUNG MV), especially Mario von Weber, for nutrient monitoring data  
and the DWD for meteorological data.

*Financial support.* This study was supported by the German Research Foundation (DFG) within the PhD graduate school  
890 “Baltic TRANSCOAST” GRK 2000/1. A. Breznikar was funded by a doctoral scholarship from the Deutsche Bundesstiftung  
Umwelt (DBU).

## References

Augustin, J. (Ed.): Gaseous emissions from constructed wetlands and (re)flooded meadows, in: International Conference:  
Constructed and Riverine Wetlands for Optimal Control of Wastewater at Catchment Scale, edited by: Mander, Ü., Vohla, C.  
895 and Poom, A., Tartu Univ. Press, 2003.

Augustin, J. and Chojnicki, B.: Austausch von klimarelevanten Spurengasen, Klimawirkung und Kohlenstoffdynamik in den  
ersten Jahren nach Wiedervernässung von degradiertem Niedermoorgrünland, Berichte des Leibniz-Institut für  
Gewässerökologie und Binnenfischerei, 50–61, 2008.

Augustin, J., Merbach, W., Steffens, L., and Snelinski, B.: Nitrous Oxide Fluxes Of Disturbed Minerotrophic Peatlands,  
900 Agribiological research (Germany), 51, 47–57, 1998.

Bange, H. W., Bartell, U. H., Rapsomanikis, S., and Andreae, M. O.: Methane in the Baltic and North Seas and a reassessment  
of the marine emissions of methane, Global Biogeochem. Cycles, 8, 465–480, <https://doi.org/10.1029/94GB02181>, 1994.

Bange, H. W., Dahlke, S., Ramesh, R., Meyer-Reil, L.-A., Rapsomanikis, S., and Andreae, M. O.: Seasonal Study of Methane  
and Nitrous Oxide in the Coastal Waters of the Southern Baltic Sea, Estuarine, Coastal and Shelf Science, 47, 807–817,  
905 <https://doi.org/10.1006/ecss.1998.0397>, 1998.

Bartlett, K. B., Bartlett, D. S., Harriss, R. C., and Sebacher, D. I.: Methane emissions along a salt marsh salinity gradient,  
Biogeochemistry, 4, 183–202, <https://doi.org/10.1007/BF02187365>, 1987.

Beldowski, J., Löffler, A., Schneider, B., and Joensuu, L.: Distribution and biogeochemical control of total CO<sub>2</sub> and total  
alkalinity in the Baltic Sea, Journal of Marine Systems, 81, 252–259, <https://doi.org/10.1016/j.jmarsys.2009.12.020>, 2010.

910 Bockholt, R.: Flächen-, Ertrags- und Problemanalyse des Überschwemmungsgrünlandes der Ostsee-, Bodden- und  
Haffgewässer, Forschungsbericht Universität Rostock, 17, 1985.

- Boetius, A., Ravensschlag, K., Schubert, C. J., Rickert, D., Widdel, F., Gieseke, A., Amann, R., Jørgensen, B. B., Witte, U., and Pfannkuche, O.: A marine microbial consortium apparently mediating anaerobic oxidation of methane, *Nature*, 407, 623–626, <https://doi.org/10.1038/35036572>, 2000.
- 915 Borges, A. V., Champenois, W., Gypens, N., Delille, B., and Harlay, J.: Massive marine methane emissions from near-shore shallow coastal areas, *Scientific reports*, 6, 27908, <https://doi.org/10.1038/srep27908>, 2016.
- Borges, A. V., Speeckaert, G., Champenois, W., Scranton, M. I., and Gypens, N.: Productivity and Temperature as Drivers of Seasonal and Spatial Variations of Dissolved Methane in the Southern Bight of the North Sea, *Ecosystems*, 21, 583–599, <https://doi.org/10.1007/s10021-017-0171-7>, 2018.
- 920 Brisch, A.: Erkundung von Torfmächtigkeit und Vegetation in zwei potenziellen Wiedervernässungsgebieten bei Ramin und Grosow (Rügen), Unpublished expert opinion by Naturschutzstiftung Deutsche Ostsee, 2015.
- Bubier, J., Crill, P., Mosedale, A., Frohling, S., and Linder, E.: Peatland responses to varying interannual moisture conditions as measured by automatic CO<sub>2</sub> chambers, *Global Biogeochem. Cycles*, 17, 1-35, <https://doi.org/10.1029/2002GB001946>, 2003.
- 925 Burgin, A. J. and Groffman, P. M.: Soil O<sub>2</sub> controls denitrification rates and N<sub>2</sub>O yield in a riparian wetland, *J. Geophys. Res.*, 117, 1–15, <https://doi.org/10.1029/2011JG001799>, 2012.
- Cabezas, A., Gelbrecht, J., Zwirnmann, E., Barth, M., and Zak, D.: Effects of degree of peat decomposition, loading rate and temperature on dissolved nitrogen turnover in rewetted fens, *Soil Biology and Biochemistry*, 48, 182–191, <https://doi.org/10.1016/j.soilbio.2012.01.027>, 2012.
- 930 Capone, D. G. and Kiene, R. P.: Comparison of microbial dynamics in marine and freshwater sediments: Contrasts in anaerobic carbon catabolism, *Limnol. Oceanogr.*, 33, 725–749, <https://doi.org/10.4319/lo.1988.33.4part2.0725>, 1988.
- Carter, B. R., Radich, J. A., Doyle, H. L., and Dickson, A. G.: An automated system for spectrophotometric seawater pH measurements, *Limnol. Oceanogr. Methods*, 11, 16–27, <https://doi.org/10.4319/lom.2013.11.16>, 2013.
- 935 Chmura, G. L., Kellman, L., and Guntenspergen, G. R.: The greenhouse gas flux and potential global warming feedbacks of a northern macrotidal and microtidal salt marsh, *Environ. Res. Lett.*, 6, 1–6, <https://doi.org/10.1088/1748-9326/6/4/044016>, 2011.
- Chmura, G. L., Kellman, L., van Ardenne, L., and Guntenspergen, G. R.: Greenhouse Gas Fluxes from Salt Marshes Exposed to Chronic Nutrient Enrichment, *PloS one*, 11, 1-13, <https://doi.org/10.1371/journal.pone.0149937>, 2016.
- Couwenberg, J., Thiele, A., Tanneberger, F., Augustin, J., Bärtsch, S., Dubovik, D., Liashchynskaya, N., Michaelis, D., Minke, M., Skuratovich, A., and Joosten, H.: Assessing greenhouse gas emissions from peatlands using vegetation as a proxy, *Hydrobiologia*, 674, 67–89, <https://doi.org/10.1007/s10750-011-0729-x>, 2011.

- Danevčič, T., Mandic-Mulec, I., Stres, B., Stopar, D., and Hacin, J.: Emissions of CO<sub>2</sub>, CH<sub>4</sub> and N<sub>2</sub>O from Southern European peatlands, *Soil Biology and Biochemistry*, 42, 1437–1446, <https://doi.org/10.1016/j.soilbio.2010.05.004>, 2010.
- Dean, J. F., Middelburg, J. J., Röckmann, T., Aerts, R., Blauw, L. G., Egger, M., Jetten, M. S. M., Jong, A. E. E. de, Meisel, O. H., Rasigraf, O., Slomp, C. P., in't Zandt, M. H., and Dolman, A. J.: Methane Feedbacks to the Global Climate System in a Warmer World, *Rev. Geophys.*, 56, 207–250, <https://doi.org/10.1002/2017RG000559>, 2018.
- Dickson, A. and Riley, J.: The estimation of acid dissociation constants in seawater media from potentiometric titrations with strong base. I. The ionic product of water — Kw, *Marine Chemistry*, 7, 89–99, [https://doi.org/10.1016/0304-4203\(79\)90001-X](https://doi.org/10.1016/0304-4203(79)90001-X), 1979.
- 950 Dickson, A. G.: Standard potential of the reaction: AgCl(s) + 1/2H<sub>2</sub>(g) = Ag(s) + HCl(aq), and the standard acidity constant of the ion HSO<sub>4</sub><sup>-</sup> in synthetic sea water from 273.15 to 318.15 K, *The Journal of Chemical Thermodynamics*, 22, 113–127, [https://doi.org/10.1016/0021-9614\(90\)90074-Z](https://doi.org/10.1016/0021-9614(90)90074-Z), 1990.
- Dickson, A. G., Sabine, C. L. and Christian, J. R. (Eds.): Guide to best practices for ocean CO<sub>2</sub> measurements, North Pacific Marine Science Organization, 2007.
- 955 Dlugokencky, E., Crotwell, A., Mund, J., Crotwell, M., and Thoning, K.: Atmospheric Methane Dry Air Mole Fractions from the NOAA ESRL Carbon Cycle Cooperative Global Air Sampling Network, 1983-2018, <https://doi.org/10.15138/wkgj-f215>, 2019b.
- Dlugokencky, E., Crotwell, A., Mund, J., Crotwell, M., and Thoning, K.: Atmospheric Methane Dry Air Mole Fractions from the NOAA ESRL Carbon Cycle Cooperative Global Air Sampling Network, 1983-2018, <https://doi.org/10.15138/VNCZ-M766>, 2019a.
- 960 Duhamel, S., Nogaro, G., and Steinman, A. D.: Effects of water level fluctuation and sediment–water nutrient exchange on phosphorus biogeochemistry in two coastal wetlands, *Aquat Sci*, 79, 57–72, <https://doi.org/10.1007/s00027-016-0479-y>, 2017.
- Edler, L.: Recommendations on Methods for Marine Biological Studies in the Baltic Sea: Phytoplankton and chlorophyll, *Baltic Marine Biologists*., 1979.
- 965 Fiedler, J., Fuß, R., Glatzel, S., Hagemann, U., Huth, V., Jordan, S., Jurasinski, G., Kutzbach, L., Maier, M., Schäfer, K., Weber, T., and Weymann, D.: Best Practice Guideline Measurement of carbon dioxide, methane and nitrous oxide fluxes between soil-vegetation-systems and the atmosphere using non-steady state chambers, <https://doi.org/10.23689/figeo-5422>, 2022.
- Fisher, J. and Acreman, M. C.: Wetland nutrient removal: a review of the evidence, *Hydrol. Earth Syst. Sci.*, 8, 673–685, <https://doi.org/10.5194/hess-8-673-2004>, 2004.
- 970

- Flessa, H., Wild, U., Klemisch, M., and Pfadenhauer, J.: Nitrous oxide and methane fluxes from organic soils under agriculture, 49, 1998.
- Fox, J. and Weisberg, S.: An {R} Companion to Applied Regression, Third Edition. Thousand Oaks CA: Sage, <https://socialsciences.mcmaster.ca/jfox/Books/Companion/> (last access: 03 April 2022), 2019.
- 975 Franz, D., Koebsch, F., Larmanou, E., Augustin, J., and Sachs, T.: High net CO<sub>2</sub> and CH<sub>4</sub> release at a eutrophic shallow lake on a formerly drained fen, *Biogeosciences*, 13, 3051–3070, <https://doi.org/10.5194/bg-13-3051-2016>, 2016.
- Gattuso, J.-P., Epitalon, J.-M., Lavigne, H., and Orr, J.: seacarb: Seawater Carbonate Chemistry, <https://CRAN.R-project.org/> <https://CRAN.R-project.org/package=seacarb> (last access: 06 February 2022), R package version 3.2.15, 2019.
- 980 Geurts, J. J. M., Smolders, A. J. P., Banach, A. M., van de Graaf, J. P. M., Roelofs, J. G. M., and Lamers, L. P. M.: The interaction between decomposition, net N and P mineralization and their mobilization to the surface water in fens, *Water research*, 44, 3487–3495, <https://doi.org/10.1016/j.watres.2010.03.030>, 2010.
- Glatzel, S., Forbrich, I., Krüger, C., Lemke, S., and Gerold, G.: Environmental controls of greenhouse gas release in a restoring peat bog in NW Germany, *Biogeosciences Discussions, European Geosciences*, 213–242, <https://doi.org/10.5194/bgd-5-213-2008>, 2008.
- 985 Glatzel, S. and Stahr, K.: Methane and nitrous oxide exchange in differently fertilised grassland in southern Germany, *Plant and Soil*, 231, 21–35, 2001.
- Goldberg, S. D., Knorr, K.-H., Blodau, C., Lischeid, G., and Gebauer, G.: Impact of altering the water table height of an acidic fen on N<sub>2</sub>O and NO fluxes and soil concentrations, *Global change biology*, 16, 220–233, <https://doi.org/10.1111/j.1365-2486.2009.02015.x>, 2010.
- 990 Grasshoff, K., Kremling, K., and Ehrhardt, M.: *Methods of Seawater Analysis*, 2009.
- Grolemund, G. and Wickham, H.: Dates and Times Made Easy with lubridate. *Journal of Statistical Software*, <https://www.jstatsoft.org/v40/i03/> (last access: 03 April 2022), 2011.
- Hahn, J., Köhler, S., Glatzel, S., and Jurasinski, G.: Methane Exchange in a Coastal Fen in the First Year after Flooding-A Systems Shift, *PloS one*, 10, 1-25, <https://doi.org/10.1371/journal.pone.0140657>, 2015.
- 995 Hahn-Schöfl, M., Zak, D., Minke, M., Gelbrecht, J., Augustin, J., and Freibauer, A.: Organic sediment formed during inundation of a degraded fen grassland emits large fluxes of CH<sub>4</sub> and CO<sub>2</sub>, *Biogeosciences*, 8, 1539–1550, <https://doi.org/10.5194/bg-8-1539-2011>, 2011.
- Harpenslager, S. F., van den Elzen, E., Kox, M. A., Smolders, A. J., Ettwig, K. F., and Lamers, L. P.: Rewetting former agricultural peatlands: Topsoil removal as a prerequisite to avoid strong nutrient and greenhouse gas emissions, *Ecological Engineering*, 84, 159–168, <https://doi.org/10.1016/j.ecoleng.2015.08.002>, 2015.
- 1000



- HELCOM: HELCOM Guidelines for the annual and periodical compilation and reporting of waterborne pollution inputs to the Baltic Sea (PLC-Water), [http://nest.su.se/helcom\\_plc/](http://nest.su.se/helcom_plc/) (last access 17 December 2021), HELCOM, 2019.
- Heyer, J. and Berger, U.: Methane Emission from the Coastal Area in the Southern Baltic Sea, *Estuarine, Coastal and Shelf Science*, 51, 13–30, <https://doi.org/10.1006/ecss.2000.0616>, 2000.
- 1005 Hogan, D. M., Jordan, T. E., and Walbridge, M. R.: Phosphorus retention and soil organic carbon in restored and natural freshwater wetlands, *Wetlands*, 24, 573–585, [https://doi.org/10.1672/0277-5212\(2004\)024\[0573:PRASOC\]2.0.CO;2](https://doi.org/10.1672/0277-5212(2004)024[0573:PRASOC]2.0.CO;2), 2004.
- Holz, R., Herrmann, C., and Müller-Motzfeld, G.: Vom Polder zum Ausdeichungsgebiet: Das Projekt Karrendorfer Wiesen und die Zukunft der Küstenüberflutungsgebiete in Mecklenburg-Vorpommern, *Natur und Naturschutz in MV, Schriftenreihe des Institutes für Landschaftsökologie und Naturschutz Greifswald, Band 32*, 1996.
- 1010 Joosten, H. and Clarke, D.: *Wise use of mires and peatlands, Background and principles including a framework for decision-making*, 2002.
- Jørgensen, B. B. (Ed.): *Bacteria and Marine Biogeochemistry*, in: *Marine Geochemistry*, [https://doi.org/10.1007/3-540-32144-6\\_5](https://doi.org/10.1007/3-540-32144-6_5), 2006.
- Jørgensen, C. J. and Elberling, B.: Effects of flooding-induced N<sub>2</sub>O production, consumption and emission dynamics on the annual N<sub>2</sub>O emission budget in wetland soil, *Soil Biology and Biochemistry*, 53, 9–17, <https://doi.org/10.1016/j.soilbio.2012.05.005>, 2012.
- Jurasinski, G., Günther, A. B., Huth, V., Couwenberg, J., and Glatzel, S.: Paludiculture – productive use of wet peatlands., *Ecosystem services provided by paludiculture – Greenhouse gas emissions*, 79–94, 2016.
- Jurasinski, G., Janssen, M., Voss, M., Böttcher, M. E., Brede, M., Burchard, H., Forster, S., Gosch, L., Gräwe, U., Gründling-  
1020 Pfaff, S., Haider, F., Ibenthal, M., Karow, N., Karsten, U., Kreuzburg, M., Lange, X., Leinweber, P., Massmann, G., Ptak, T., Rezanezhad, F., Rehder, G., Romoth, K., Schade, H., Schubert, H., Schulz-Vogt, H., Sokolova, I. M., Strehse, R., Unger, V., Westphal, J., and Lennartz, B.: Understanding the Coastal Ecocline: Assessing Sea–Land Interactions at Non-tidal, Low-Lying Coasts Through Interdisciplinary Research, *Front. Mar. Sci.*, 5, <https://doi.org/10.3389/fmars.2018.00342>, 2018.
- Jurasinski, G., Koebsch, F., Guenther, A., and Beetz, S.: Flux rate calculation from dynamic closed chamber measurements.,  
1025 <https://CRAN.R-project.org/package=flux> (last access: 06 February 2022), R package version 0.3-0, 2014.
- Kaat, A. and Joosten, H.: *Factbook for UNFCCC policies on peat carbon emissions*, 2009.
- Kandel, T. P., Lærke, P. E., Hoffmann, C. C., and Elsgaard, L.: Complete annual CO<sub>2</sub>, CH<sub>4</sub>, and N<sub>2</sub>O balance of a temperate riparian wetland 12 years after rewetting, *Ecological Engineering*, 127, 527–535, <https://doi.org/10.1016/j.ecoleng.2017.12.019>, 2019.

- 1030 Knittel, K. and Boetius, A.: Anaerobic oxidation of methane: progress with an unknown process, *Annual review of microbiology*, 63, 311–334, <https://doi.org/10.1146/annurev.micro.61.080706.093130>, 2009.
- Koebisch, F., Glatzel, S., Hofmann, J., Forbrich, I., and Jurasinski, G.: CO<sub>2</sub> exchange of a temperate fen during the conversion from moderately rewetted to flooding, *J. Geophys. Res. Biogeosci.*, 118, 940–950, <https://doi.org/10.1002/jgrg.20069>, 2013.
- Koebisch, F., Gottschalk, P., Beyer, F., Wille, C., Jurasinski, G., and Sachs, T.: The impact of occasional drought periods on  
1035 vegetation spread and greenhouse gas exchange in rewetted fens, *Philosophical transactions of the Royal Society of London. Series B, Biological sciences*, 375, 20190685, <https://doi.org/10.1098/rstb.2019.0685>, 2020.
- Koebisch, F., Jurasinski, G., Koch, M., Hofmann, J., and Glatzel, S.: Controls for multi-scale temporal variation in ecosystem methane exchange during the growing season of a permanently inundated fen, *Agricultural and Forest Meteorology*, 204, 94–105, <https://doi.org/10.1016/j.agrformet.2015.02.002>, 2015.
- 1040 Koebisch, F., Winkel, M., Liebner, S., Liu, B., Westphal, J., Schmiedinger, I., Spitzzy, A., Gehre, M., Jurasinski, G., Köhler, S., Unger, V., Koch, M., Sachs, T., and Böttcher, M. E.: Sulfate deprivation triggers high methane production in a disturbed and rewetted coastal peatland, *Biogeosciences*, 16, 1937–1953, <https://doi.org/10.5194/bg-16-1937-2019>, 2019.
- Kool, D. M., Dolfing, J., Wrage, N., and van Groenigen, J. W.: Nitrifier denitrification as a distinct and significant source of nitrous oxide from soil, *Soil Biology and Biochemistry*, 43, 174–178, <https://doi.org/10.1016/j.soilbio.2010.09.030>, 2011.
- 1045 Kreyling, J., Tanneberger, F., Jansen, F., van der Linden, S., Aggenbach, C., Blüml, V., Couwenberg, J., Emsens, W.-J., Joosten, H., Klimkowska, A., Kotowski, W., Kozub, L., Lennartz, B., Liczner, Y., Liu, H., Michaelis, D., Oehmke, C., Parakenings, K., Pleyl, E., Poyda, A., Raabe, S., Röhl, M., Rücker, K., Schneider, A., Schrautzer, J., Schröder, C., Schug, F., Seeber, E., Thiel, F., Thiele, S., Tiemeyer, B., Timmermann, T., Urich, T., van Diggelen, R., Vegelin, K., Verbruggen, E., Wilmking, M., Wrage-Mönnig, N., Wołajko, L., Zak, D., and Jurasinski, G.: Rewetting does not return drained fen peatlands  
1050 to their old selves, *Nature communications*, 12, 5693, <https://doi.org/10.1038/s41467-021-25619-y>, 2021.
- Kuliński, K., Rehder, G., Asmala, E., Bartosova, A., Carstensen, J., Gustafsson, B., Hall, P. O. J., Humborg, C., Jilbert, T., Jürgens, K., Meier, H. E. M., Müller-Karulis, B., Naumann, M., Olesen, J. E., Savchuk, O., Schramm, A., Slomp, C. P., Sofiev, M., Sobek, A., Szymczycha, B., and Undeman, E.: Biogeochemical functioning of the Baltic Sea, *Earth Syst. Dynam.*, 13, 633–685, <https://doi.org/10.5194/esd-13-633-2022>, 2022.
- 1055 Kuliński, K., Schneider, B., Hammer, K., Machulik, U., and Schulz-Bull, D.: The influence of dissolved organic matter on the acid–base system of the Baltic Sea, *Journal of Marine Systems*, 132, 106–115, <https://doi.org/10.1016/j.jmarsys.2014.01.011>, 2014.
- Kuliński, K., Schneider, B., Szymczycha, B., and Stokowski, M.: Structure and functioning of the acid–base system in the Baltic Sea, *Earth Syst. Dynam.*, 8, 1107–1120, <https://doi.org/10.5194/esd-8-1107-2017>, 2017.

- 1060 Lamers, L. P., Smolders, A. J., and Roelofs, J. G.: The restoration of fens in the Netherlands, *Hydrobiologia*, 478, 107–130, <https://doi.org/10.1023/A:1021022529475>, 2002.
- Lennartz, B. and Liu, H.: Hydraulic Functions of Peat Soils and Ecosystem Service, *Front. Environ. Sci.*, 7, <https://doi.org/10.3389/fenvs.2019.00092>, 2019.
- Leppelt, T., Dechow, R., Gebbert, S., Freibauer, A., Lohila, A., Augustin, J., Drösler, M., Fiedler, S., Glatzel, S., Höper, H.,  
1065 Järveoja, J., Lærke, P. E., Maljanen, M., Mander, Ü., Mäkiranta, P., Minkkinen, K., Ojanen, P., Regina, K., and Strömngren, M.: Nitrous oxide emission budgets and land-use-driven hotspots for organic soils in Europe, *Biogeosciences*, 11, 6595–6612, <https://doi.org/10.5194/bg-11-6595-2014>, 2014.
- Liu, H. and Lennartz, B.: Short Term Effects of Salinization on Compound Release from Drained and Restored Coastal Wetlands, *Water*, 11, 1549, <https://doi.org/10.3390/w11081549>, 2019.
- 1070 Liu, H., Zak, D., Rezanezhad, F., and Lennartz, B.: Soil degradation determines release of nitrous oxide and dissolved organic carbon from peatlands, *Environ. Res. Lett.*, 14, 94009, <https://doi.org/10.1088/1748-9326/ab3947>, 2019.
- Livingston, G. P. and Hutchinson, G.: Enclosure-based measurement of trace gas exchange: applications and sources of error., In: Matson, P.A. and Harris, R.C., Eds., *Biogenic trace gases: measuring emissions from soil and water.*, Blackwell Science Ltd., Oxford, UK., 14–51, 1995.
- 1075 Löffler, A., Schneider, B., Perttilä, M., and Rehder, G.: Air–sea CO<sub>2</sub> exchange in the Gulf of Bothnia, Baltic Sea, *Continental Shelf Research*, 37, 46–56, <https://doi.org/10.1016/j.csr.2012.02.002>, 2012.
- Martikainen, P. J., Nykänen, H., Crill, P., and Silvola, J.: Effect of a lowered water table on nitrous oxide fluxes from northern peatlands, *Nature*, 366, 51–53, <https://doi.org/10.1038/366051a0>, 1993.
- Millero, F. J.: Carbonate constants for estuarine waters, *Mar. Freshwater Res.*, 61, 139, <https://doi.org/10.1071/MF09254>,  
1080 2010.
- Minkkinen, K., Ojanen, P., Koskinen, M., and Penttilä, T.: Nitrous oxide emissions of undrained, forestry-drained, and rewetted boreal peatlands, *Forest Ecology and Management*, 478, 118494, <https://doi.org/10.1016/j.foreco.2020.118494>, 2020.
- Moore, T. R., Roulet, N. T., and Waddington, J. M.: Uncertainty in Predicting the Effect of Climatic Change on the Carbon Cycling of Canadian Peatlands, *Climatic Change*, 40, 229–245, <https://doi.org/10.1023/A:1005408719297>, 1998.
- 1085 Moseman-Valtierra, S., Gonzalez, R., Kroeger, K. D., Tang, J., Chao, W. C., Crusius, J., Bratton, J., Green, A., and Shelton, J.: Short-term nitrogen additions can shift a coastal wetland from a sink to a source of N<sub>2</sub>O, *Atmospheric Environment*, 45, 4390–4397, <https://doi.org/10.1016/j.atmosenv.2011.05.046>, 2011.

- Müller, J. D., Bastkowski, F., Sander, B., Seitz, S., Turner, D. R., Dickson, A. G., and Rehder, G.: Metrology for pH Measurements in Brackish Waters—Part 1: Extending Electrochemical pH Measurements of TRIS Buffers to Salinities 5–20, *Front. Mar. Sci.*, 5, <https://doi.org/10.3389/fmars.2018.00176>, 2018.
- Müller, J. D. and Rehder, G.: Metrology of pH Measurements in Brackish Waters—Part 2: Experimental Characterization of Purified meta-Cresol Purple for Spectrophotometric pH Measurements, *Front. Mar. Sci.*, 5, <https://doi.org/10.3389/fmars.2018.00177>, 2018.
- Müller, J. D., Schneider, B., and Rehder, G.: Long-term alkalinity trends in the Baltic Sea and their implications for CO<sub>2</sub>-induced acidification, *Limnol. Oceanogr.*, 61, 1984–2002, <https://doi.org/10.1002/lno.10349>, 2016.
- Neubauer, S. C., Franklin, R. B., and Berrier, D. J.: Saltwater intrusion into tidal freshwater marshes alters the biogeochemical processing of organic carbon, *Biogeosciences*, 10, 8171–8183, <https://doi.org/10.5194/bg-10-8171-2013>, 2013.
- Oertel, C., Matschullat, J., Zurba, K., Zimmermann, F., and Erasmi, S.: Greenhouse gas emissions from soils—A review, *Geochemistry*, 76, 327–352, <https://doi.org/10.1016/j.chemer.2016.04.002>, 2016.
- Oremland, R. S. (Ed.): The biogeochemistry of methanogenic bacteria, in: The biology of microorganisms. Available online at <http://pubs.er.usgs.gov/publication/70198767>, 1988.
- Parish, F.: Assessment on peatlands, biodiversity and climate change, Main report, 2008.
- Pedersen, T. L.: patchwork: The Composer of Plots. R package version 1.1.1, <https://CRAN.R-project.org/package=patchwork>, 2020.
- Petersen, S. O., Hoffmann, C. C., Schäfer, C.-M., Blicher-Mathiesen, G., Elsgaard, L., Kristensen, K., Larsen, S. E., Torp, S. B., and Greve, M. H.: Annual emissions of CH<sub>4</sub> and N<sub>2</sub>O, and ecosystem respiration, from eight organic soils in Western Denmark managed by agriculture, *Biogeosciences*, 9, 403–422, <https://doi.org/10.5194/bg-9-403-2012>, 2012.
- Pönisch, D. L.: Methodenentwicklung und –anwendung zur Analytik von Methan und Lachgas in Seewasser, Leibniz Institute for Baltic Sea Research Warnemünde (IOW), Master thesis, 2018.
- Rassamee, V., Sattayatewa, C., Pagilla, K., and Chandran, K.: Effect of oxic and anoxic conditions on nitrous oxide emissions from nitrification and denitrification processes, *Biotechnology and bioengineering*, 108, 2036–2045, <https://doi.org/10.1002/bit.23147>, 2011.
- Reeburgh, W. S.: Oceanic methane biogeochemistry, *Chemical reviews*, 107, 486–513, <https://doi.org/10.1021/cr050362v>, 2007.
- Regina, K., Nykänen, H., Silvola, J., and Martikainen, P. J.: Fluxes of nitrous oxide from boreal peatlands as affected by peatland type, water table level and nitrification capacity, *Biogeochemistry*, 35, 401–418, <https://doi.org/10.1007/BF02183033>, 1996.

- Regina, K., Silvola, J., and Martikainen, P. J.: Short-term effects of changing water table on N<sub>2</sub>O fluxes from peat monoliths from natural and drained boreal peatlands, *Global change biology*, 5, 183–189, <https://doi.org/10.1046/j.1365-2486.1999.00217.x>, 1999.
- 1120
- Richert, M., Dietrich, O., Koppisch, D., and Roth, S.: The Influence of Rewetting on Vegetation Development and Decomposition in a Degraded Fen, *Restor Ecology*, 8, 186–195, <https://doi.org/10.1046/j.1526-100x.2000.80026.x>, 2000.
- Roughan, B. L., Kellman, L., Smith, E., and Chmura, G. L.: Nitrous oxide emissions could reduce the blue carbon value of marshes on eutrophic estuaries, *Environ. Res. Lett.*, 13, 44034, <https://doi.org/10.1088/1748-9326/aab63c>, 2018.
- 1125
- Rysgaard, S., Thastum, P., Dalsgaard, T., Christensen, P. B., Sloth, N. P., and Rysgaard, S.: Effects of Salinity on NH<sub>4</sub><sup>+</sup> Adsorption Capacity, Nitrification, and Denitrification in Danish Estuarine Sediments, *Estuaries*, 22, 21, <https://doi.org/10.2307/1352923>, 1999.
- Sabbaghzadeh, B., Arévalo-Martínez, D. L., Glockzin, M., Otto, S., and Rehder, G.: Meridional and Cross-Shelf Variability of N<sub>2</sub>O and CH<sub>4</sub> in the Eastern-South Atlantic, *J. Geophys. Res. Oceans*, 126, <https://doi.org/10.1029/2020JC016878>, 2021.
- 1130
- Schneider, B. and Müller, J. D.: Biogeochemical Transformations in the Baltic Sea, <https://doi.org/10.1007/978-3-319-61699-5>, 2018.
- Schönheit, P., Kristjansson, J. K., and Thauer, R. K.: Kinetic mechanism for the ability of sulfate reducers to out-compete methanogens for acetate, *Archives of microbiology*, 132, 285–288, 1982.
- Segarra, K. E., Comerford, C., Slaughter, J., and Joye, S. B.: Impact of electron acceptor availability on the anaerobic oxidation of methane in coastal freshwater and brackish wetland sediments, *Geochimica et Cosmochimica Acta*, 115, 15–30, <https://doi.org/10.1016/j.gca.2013.03.029>, 2013.
- 1135
- Segers, R. and Kengen, S.: Methane production as a function of anaerobic carbon mineralization: A process model, *Soil Biology and Biochemistry*, 30, 1107–1117, [https://doi.org/10.1016/S0038-0717\(97\)00198-3](https://doi.org/10.1016/S0038-0717(97)00198-3), 1998.
- Seifert, T., Tauber, F., and Kayser, B.: A high resolution spherical grid topography of the Baltic Sea – 2nd edition, *Baltic Sea Science Congress, Stockholm 25-29. November 2001, Poster #147*, 2001.
- 1140
- Smolders, A. J. P., Lamers, L. P. M., Lucassen, E. C. H. E. T., van der Velde, G., and Roelofs, J. G. M.: Internal eutrophication: How it works and what to do about it—a review, *Chemistry and Ecology*, 22, 93–111, <https://doi.org/10.1080/02757540600579730>, 2006.
- Steinle, L., Maltby, J., Treude, T., Kock, A., Bange, H. W., Engbersen, N., Zopfi, J., Lehmann, M. F., and Niemann, H.: Effects of low oxygen concentrations on aerobic methane oxidation in seasonally hypoxic coastal waters, *Biogeosciences*, 14, 1631–1645, <https://doi.org/10.5194/bg-14-1631-2017>, 2017.
- 1145

- Steinmuller, H. E. and Chambers, L. G.: Can Saltwater Intrusion Accelerate Nutrient Export from Freshwater Wetland Soils? An Experimental Approach, *Soil Sci. Soc. Am. j.*, 82, 283–292, <https://doi.org/10.2136/sssaj2017.05.0162>, 2018.
- Strack, M. (Ed.): *Peatlands and climate change*, Internat. Peat Soc, 2008.
- 1150 Succow, M. and Joosten, H. (Eds.): *Landschaftsökologische Moorkunde*, E. Schweizerbart'sche Verlagsbuchhandlung (Nägele u. Obermiller), 2001.
- Thomas, H. and Schneider, B.: The seasonal cycle of carbon dioxide in Baltic Sea surface waters, *Journal of Marine Systems*, 22, 53–67, [https://doi.org/10.1016/S0924-7963\(99\)00030-5](https://doi.org/10.1016/S0924-7963(99)00030-5), 1999.
- 1155 Treude, T., Krüger, M., Boetius, A., and Jørgensen, B. B.: Environmental control on anaerobic oxidation of methane in the gassy sediments of Eckernförde Bay (German Baltic), *Limnol. Oceanogr.*, 50, 1771–1786, <https://doi.org/10.4319/lo.2005.50.6.1771>, 2005.
- van de Riet, B. P., Hefting, M. M., and Verhoeven, J. T. A.: Rewetting Drained Peat Meadows: Risks and Benefits in Terms of Nutrient Release and Greenhouse Gas Exchange, *Water Air Soil Pollut. (Water, Air, & Soil Pollution)*, 224, <https://doi.org/10.1007/s11270-013-1440-5>, 2013.
- 1160 Voss, M., Deutsch, B., Liskow, I., Pastuszek, M., Schulte, U., and Sitek, S.: Nitrogen retention in the Szczecin Lagoon, Baltic Sea, *Isotopes in environmental and health studies*, 46, 355–369, <https://doi.org/10.1080/10256016.2010.503895>, 2010.
- Wang, M., Liu, H., and Lennartz, B.: Microtopography effects on carbon accumulation and nutrient release from rewetted coastal wetlands., AGU2021 Fall Meeting, 2021.
- 1165 Wanninkhof, R.: Relationship between wind speed and gas exchange over the ocean revisited, *Limnol. Oceanogr. Methods*, 12, 351–362, <https://doi.org/10.4319/lom.2014.12.351>, 2014.
- Weiss, R. F. and Price, B. A.: Nitrous oxide solubility in water and seawater, *Marine Chemistry*, 8, 347–359, [https://doi.org/10.1016/0304-4203\(80\)90024-9](https://doi.org/10.1016/0304-4203(80)90024-9), 1980.
- 1170 Wickham, H., Averick, M., Bryan, J., Chang, W., McGowan, L. D., François, R., Grolemond, G., Hayes, A., Henry, L., Hester, J., Kuhn, M., Pedersen, T. L., Miller, E., Bache, S. M., Müller, K., Ooms, J., Robinson, D., Seidel, D. P., Spinu, V., Takahashi, K., Vaughan, D., Wilke, C., Woo, K., and Yutani, H.: Welcome to the tidyverse. *Journal of Open Source Software*, <https://doi.org/10.21105/joss.01686>, 2019.
- Wolf-Gladrow, D. A., Zeebe, R. E., Klaas, C., Körtzinger, A., and Dickson, A. G.: Total alkalinity: The explicit conservative expression and its application to biogeochemical processes, *Marine Chemistry*, 106, 287–300, <https://doi.org/10.1016/j.marchem.2007.01.006>, 2007.
- 1175 Zak, D. and Gelbrecht, J.: The mobilisation of phosphorus, organic carbon and ammonium in the initial stage of fen rewetting (a case study from NE Germany), *Biogeochemistry*, 85, 141–151, <https://doi.org/10.1007/s10533-007-9122-2>, 2007.

Zak, D., Meyer, N., Cabezas, A., Gelbrecht, J., Mauersberger, R., Tiemeyer, B., Wagner, C., and McInnes, R.: Topsoil removal to minimize internal eutrophication in rewetted peatlands and to protect downstream systems against phosphorus pollution: A case study from NE Germany, *Ecological Engineering*, 103, 488–496, <https://doi.org/10.1016/j.ecoleng.2015.12.030>, 2017.

1180 Zielinski, T., Sagan, I. and Surosz, W. (Eds.): *Interdisciplinary Approaches for Sustainable Development Goals*, Springer International Publishing, <https://doi.org/10.1007/978-3-319-71788-3>, 2018.